Published OnlineFirst November 22, 2013; DOI: 10.1158/0008-5472.CAN-13-1836

In conclusion, this study demonstrated the tumor-suppressive effects and major underlying mechanism of efatutazone involving inactivation of the Akt pathway. Treatment with efatutazone combined with cetuximab produced a synergistic effect by negatively regulating both the PI3K–Akt and MAPK pathways. These results suggest that efatutazone could be used both alone and in combination with cetuximab as a potential therapeutic approach for ESCC.

Disclosure of Potential Conflicts of Interest

No potential conflicts of interest were disclosed.

Authors' Contributions

Conception and design: H. Sawayama, T. Ishimoto, J. Kurashige, Y. Shiose, Hideo Baba

Development of methodology: H. Sawayama, T. Ishimoto, J. Kurashige, K. Hirashima

Acquisition of data (provided animals, acquired and managed patients, provided facilities, etc.): H. Sawayama, T. Ishimoto, M. Watanabe, N. Yoshida

Analysis and interpretation of data (e.g., statistical analysis, biostatistics, computational analysis): H. Sawayama, T. Ishimoto, M. Watanabe

Writing, review, and/or revision of the manuscript: H. Sawayama, T. Ishimoto, Y. Shiose

Administrative, technical, or material support (i.e., reporting or organizing data, constructing databases): H. Sugihara, Y. Shiose

Study supervision: M. Watanabe, M. Iwatsuki, Y. Baba, E. Oki, M. Morita, Hideo Baba

Acknowledgments

The authors thank Drs. Youhei Tanaka, Hironobu Shigaki, Hirohisa Okabe, Koichi Kinoshita, Seiya Saito, and Yukiharu Hiyoshi for their valuable research advice, Naomi Yokoyama, Kenichi Yamaguchi, and Keisuke Miyake for technical assistance, and Dr. Kenichi Iyama for providing the pathological diagnoses.

Grant Support

This work was supported in part by the scholarship for the Graduate School of Medical Sciences, Kumamoto University, Japan.

The costs of publication of this article were defrayed in part by the payment of page charges. This article must therefore be hereby marked *advertisement* in accordance with 18 U.S.C. Section 1734 solely to indicate this fact.

Received July 4, 2013; revised October 16, 2013; accepted November 3, 2013; published OnlineFirst November 22, 2013.

References

1. Michalik L, Desvergne B, Wahli W. Peroxisome-proliferator-activated receptors and cancers: complex stories. Nat Rev Cancer 2004;4:61–70.
2. Tontonoz P, Hu E, Spiegelman BM. Stimulation of adipogenesis in fibroblasts by PPAR gamma 2, a lipid-activated transcription factor. Cell 1994;79:1147–56.
3. Rosen ED, Spiegelman BM. PPARgamma: a nuclear regulator of metabolism, differentiation, and cell growth. J Biol Chem 2001;276:37731–4.
4. Copland JA, Marlow LA, Kurakata S, Fujiwara K, Wong AK, Kreinest PA, et al. Novel high-affinity PPARgamma agonist alone and in combination with paclitaxel inhibits human anaplastic thyroid carcinoma tumor growth via p21WAF1/CIP1. Oncogene 2006;25:2304–17.
5. Marlow LA, Reynolds LA, Cleland AS, Cooper SJ, Gumz ML, Kurakata S, et al. Reactivation of suppressed RhoB is a critical step for the inhibition of anaplastic thyroid cancer growth. Cancer Res 2009;69:1536–44.
6. Motomura W, Okumura T, Takahashi N, Obara T, Kohgo Y. Activation of peroxisome proliferator-activated receptor gamma by troglitazone inhibits cell growth through the increase of p27KiP1 in human. Pancreatic carcinoma cells. Cancer Res 2000;60:5558–64.
7. Yu J, Qiao L, Zimmermann L, Ebert MP, Zhang H, Lin W, et al. Troglitazone inhibits tumor growth in hepatocellular carcinoma *in vitro* and *in vivo*. Hepatology 2006;43:134–43.
8. Nemenoff RA, Weiser-Evans M, Winn RA. Activation and molecular targets of peroxisome proliferator-activated receptor-gamma ligands in lung cancer. PPAR Research 2008;2008:156875.
9. Du H, Chen X, Zhang J, Chen C. Inhibition of COX-2 expression by endocannabinoid 2-arachidonoylglycerol is mediated via PPAR-gamma. Br J Pharmacol 2011;163:1533–49.
10. Yang WL, Frucht H. Activation of the PPAR pathway induces apoptosis and COX-2 inhibition in HT-29 human colon cancer cells. Carcinogenesis 2001;22:1379–83.
11. Nicol CJ, Yoon M, Ward JM, Yamashita M, Fukamachi K, Peters JM, et al. PPARgamma influences susceptibility to DMBA-induced mammary, ovarian and skin carcinogenesis. Carcinogenesis 2004;25:1747–55.
12. Mueller E, Smith M, Sarraf P, Kroll T, Aiyer A, Kaufman DS, et al. Effects of ligand activation of peroxisome proliferator-activated receptor gamma in human prostate cancer. Proc Natl Acad Sci U S A 2000;97:10990–5.
13. Sarraf P, Mueller E, Smith WM, Wright HM, Kum JB, Aaltonen LA, et al. Loss-of-function mutations in PPAR gamma associated with human colon cancer. Mol Cell 1999;3:799–804.
14. Forman BM, Tontonoz P, Chen J, Brun RP, Spiegelman BM, Evans RM. 15-Deoxy-delta 12, 14-prostaglandin J2 is a ligand for the adipocyte determination factor PPAR gamma. Cell 1995;83:803–12.
15. Lehmann JM, Moore LB, Smith-Oliver TA, Wilkison WO, Willson TM, Kliewer SA. An antidiabetic thiazolidinedione is a high affinity ligand for peroxisome proliferator-activated receptor gamma (PPAR gamma). J Biol Chem 1995;270:12953–6.
16. Saltiel AR, Olefsky JM. Thiazolidinediones in the treatment of insulin resistance and type II diabetes. Diabetes 1996;45:1661–9.
17. Osawa E, Nakajima A, Wada K, Ishimine S, Fujisawa N, Kawamori T, et al. Peroxisome proliferator-activated receptor gamma ligands suppress colon carcinogenesis induced by azoxymethane in mice. Gastroenterology 2003;124:361–7.
18. Sarraf P, Mueller E, Jones D, King FJ, DeAngelo DJ, Partridge JB, et al. Differentiation and reversal of malignant changes in colon cancer through PPARgamma. Nat Med 1998;4:1046–52.
19. Suh N, Wang Y, Williams CR, Risingsong R, Gilmer T, Willson TM, et al. A new ligand for the peroxisome proliferator-activated receptor-gamma (PPAR-gamma), GW7845, inhibits rat mammary carcinogenesis. Cancer Res 1999;59:5671–3.
20. Kulke MH, Demetri GD, Sharpless NE, Ryan DP, Shivdasani R, Clark JS, et al. A phase II study of troglitazone, an activator of the PPARgamma receptor, in patients with chemotherapy-resistant metastatic colorectal cancer. Cancer J 2002;8:395–9.
21. Smith MR, Manola J, Kaufman DS, George D, Oh WK, Mueller E, et al. Rosiglitazone versus placebo for men with prostate carcinoma and a rising serum prostate-specific antigen level after radical prostatectomy and/or radiation therapy. Cancer 2004;101:1569–74.
22. Pishvaian MJ, Marshall JL, Wagner AJ, Hwang JJ, Malik S, Cotarla I, et al. A phase 1 study of efatutazone, an oral peroxisome proliferator-activated receptor gamma agonist, administered to patients with advanced malignancies. Cancer 2012;118:5403–13.
23. Girnun GD, Naseri E, Vafai SB, Qu L, Szwaya JD, Bronson R, et al. Synergy between PPARgamma ligands and platinum-based drugs in cancer. Cancer Cell 2007;11:395–406.
24. Shimazaki N, Togashi N, Hanai M, Isoyama T, Wada K, Fujita T, et al. Anti-tumour activity of CS-7017, a selective peroxisome proliferator-activated receptor gamma agonist of thiazolidinedione class, in human tumour xenografts and a syngeneic tumour implant model. Eur J Cancer 2008;44:1734–43.
25. Pennathur A, Gibson MK, Jobe BA, Luketich JD. Oesophageal carcinoma. Lancet 2013;381:400–12.

Published OnlineFirst November 22, 2013; DOI: 10.1158/0008-5472.CAN-13-1836

26. Mariette C, Piessen G, Triboulet JP. Therapeutic strategies in oesophageal carcinoma: role of surgery and other modalities. Lancet Oncol 2007;8:545–53.
27. Sjoquist KM, Burmeister BH, Smithers BM, Zalcberg JR, Simes RJ, Barbour A, et al. Survival after neoadjuvant chemotherapy or chemoradiotherapy for resectable oesophageal carcinoma: an updated meta-analysis. Lancet Oncol 2011;12:681–92.
28. Bonner JA, Harari PM, Giralt J, Azarnia N, Shin DM, Cohen RB, et al. Radiotherapy plus cetuximab for squamous-cell carcinoma of the head and neck. N Engl J Med 2006;354:567–78.
29. Bonner JA, Harari PM, Giralt J, Cohen RB, Jones CU, Sur RK, et al. Radiotherapy plus cetuximab for locoregionally advanced head and neck cancer: 5-year survival data from a phase 3 randomised trial, and relation between cetuximab-induced rash and survival. Lancet Oncol 2010;11:21–8.
30. Hirashima K, Baba Y, Watanabe M, Karashima RI, Sato N, Imamura Y, et al. Aberrant activation of the mTOR pathway and anti-tumour effect of everolimus on oesophageal squamous cell carcinoma. Br J Cancer 2012;106:876–82.
31. Terashita Y, Sasaki H, Haruki N, Nishiwaki T, Ishiguro H, Shibata Y, et al. Decreased peroxisome proliferator-activated receptor gamma gene expression is correlated with poor prognosis in patients with esophageal cancer. Jpn J Clin Oncol 2002;32:238–43.
32. Wang W, Wang R, Zhang Z, Li D, Yut Y. Enhanced PPAR-gamma expression may correlate with the development of Barrett's esophagus and esophageal adenocarcinoma. Oncology Res 2011;19:141–7.
33. Takashima T, Fujiwara Y, Higuchi K, Arakawa T, Yano Y, Hasuma T, et al. PPAR-gamma ligands inhibit growth of human esophageal adenocarcinoma cells through induction of apoptosis, cell cycle arrest and reduction of ornithine decarboxylase activity. Int J Oncol 2001; 19:465–71.
34. Mabuchi S, Altomare DA, Cheung M, Zhang L, Poulikakos PI, Hensley HH, et al. RAD001 inhibits human ovarian cancer cell proliferation, enhances cisplatin-induced apoptosis, and prolongs survival in an ovarian cancer model. Clin Cancer Res 2007;13:4261–70.
35. Ogino S, Shima K, Baba Y, Nosho K, Irahara N, Kure S, et al. Colorectal cancer expression of peroxisome proliferator-activated receptor gamma (PPARG, PPARgamma) is associated with good prognosis. Gastroenterology 2009;136:1242–50.
36. Shimada T, Kojima K, Yoshiura K, Hiraishi H, Terano A. Characteristics of the peroxisome proliferator activated receptor gamma (PPAR-gamma) ligand induced apoptosis in colon cancer cells. Gut 2002; 50:658–64.
37. Degenhardt T, Saramaki A, Malinen M, Rieck M, Vaisanen S, Huotari A, et al. Three members of the human pyruvate dehydrogenase kinase gene family are direct targets of the peroxisome proliferator-activated receptor beta/delta. J Mol Biol 2007;372:341–55.
38. Carracedo A, Weiss D, Leliaert AK, Bhasin M, de Boer VC, Laurent G, et al. A metabolic prosurvival role for PML in breast cancer. J Clin Invest 2012;122:3088–100.
39. Lu Z, Hunter T. Ubiquitylation and proteasomal degradation of the p21 (Cip1), p27(Kip1) and p57(Kip2) CDK inhibitors. Cell Cycle 2010;9: 2342–52.
40. Zhou BP, Liao Y, Xia W, Spohn B, Lee MH, Hung MC. Cytoplasmic localization of p21Cip1/WAF1 by Akt-induced phosphorylation in HER-2/neu-overexpressing cells. Nat Cell Biol 2001;3:245–52.
41. Takashima T, Fujiwara Y, Hamaguchi M, Sasaki E, Tominaga K, Watanabe T, et al. Relationship between peroxisome proliferator-activated receptor-gamma expression and differentiation of human esophageal squamous cell carcinoma. Oncology Reports 2005;13: 601–6.
42. Jung YS, Qian Y, Chen X. Examination of the expanding pathways for the regulation of p21 expression and activity. Cell Signal 2010;22: 1003–12.
43. Xia W, Chen JS, Zhou X, Sun PR, Lee DF, Liao Y, et al. Phosphorylation/cytoplasmic localization of p21Cip1/WAF1 is associated with HER2/neu overexpression and provides a novel combination predictor for poor prognosis in breast cancer patients. Clin Cancer Res 2004;10: 3815–24.
44. Lito P, Pratilas CA, Joseph EW, Tadi M, Halilovic E, Zubrowski M, et al. Relief of profound feedback inhibition of mitogenic signaling by RAF inhibitors attenuates their activity in BRAFV600E melanomas. Cancer Cell 2012;22:668–82.
45. Montero-Conde C, Ruiz-Llorente S, Dominguez JM, Knauf JA, Viale A, Sherman EJ, et al. Relief of feedback inhibition of HER3 transcription by RAF and MEK inhibitors attenuates their antitumor effects in BRAF-mutant thyroid carcinomas. Cancer Discov 2013; 3:520–33.
46. Prahallad A, Sun C, Huang S, Di Nicolantonio F, Salazar R, Zecchin D, et al. Unresponsiveness of colon cancer to BRAF(V600E) inhibition through feedback activation of EGFR. Nature 2012;483: 100–3.
47. Endo Y, Suzuki M, Yamada H, Horita S, Kunimi M, Yamazaki O, et al. Thiazolidinediones enhance sodium-coupled bicarbonate absorption from renal proximal tubules via PPARgamma-dependent nongenomic signaling. Cell Metab 2011;13:550–61.

OPEN ACCESS Freely available online

PLOS ONE

Rad9, Rad17, TopBP1 and Claspin Play Essential Roles in Heat-Induced Activation of ATR Kinase and Heat Tolerance

Munkhbold Tuul[1,2], Hiroyuki Kitao[1,3]*, Makoto Iimori[1], Kazuaki Matsuoka[3,4], Shinichi Kiyonari[3], Hiroshi Saeki[2], Eiji Oki[2], Masaru Morita[2], Yoshihiko Maehara[2,3]

1 Department of Molecular Oncology, Graduate School of Medical Sciences, Kyushu University, Fukuoka, Japan, **2** Department of Surgery and Science, Graduate School of Medical Sciences, Kyushu University, Fukuoka, Japan, **3** Innovative anticancer strategy for therapeutics and diagnosis group, Innovation Center for Medical Redox Navigation, Kyushu University, Fukuoka, Japan, **4** Tokushima Research Center, Taiho Pharmaceutical Co., Ltd., Tokushima, Japan

Abstract

Hyperthermia is widely used to treat patients with cancer, especially in combination with other treatments such as radiation therapy. Heat treatment *per se* activates DNA damage responses mediated by the ATR-Chk1 and ATM-Chk2 pathways but it is not fully understood how these DNA damage responses are activated and affect heat tolerance. By performing a genetic analysis of human HeLa cells and chicken B lymphoma DT40 cells, we found that heat-induced Chk1 Ser345 phosphorylation by ATR was largely dependent on Rad9, Rad17, TopBP1 and Claspin. Activation of the ATR-Chk1 pathway by heat, however, was not associated with FancD2 monoubiquitination or RPA32 phosphorylation, which are known as downstream events of ATR kinase activation when replication forks are stalled. Downregulation of *ATR, Rad9, Rad17, TopBP1* or *Claspin* drastically reduced clonogenic cell viability upon hyperthermia, while gene knockout or inhibition of ATM kinase reduced clonogenic viability only modestly. Suppression of the ATR-Chk1 pathway activation enhanced heat-induced phosphorylation of Chk2 Thr68 and simultaneous inhibition of ATR and ATM kinases rendered severe heat cytotoxicity. These data indicate that essential factors for activation of the ATR-Chk1 pathway at stalled replication forks are also required for heat-induced activation of ATR kinase, which predominantly contributes to heat tolerance in a non-overlapping manner with ATM kinase.

Citation: Tuul M, Kitao H, Iimori M, Matsuoka K, Kiyonari S, et al. (2013) Rad9, Rad17, TopBP1 and Claspin Play Essential Roles in Heat-Induced Activation of ATR Kinase and Heat Tolerance. PLoS ONE 8(2): e55361. doi:10.1371/journal.pone.0055361

Editor: Yoshiaki Tsuji, North Carolina State University, United States of America

Received August 31, 2012; **Accepted** December 21, 2012; **Published** February 1, 2013

Funding: This work was supported in part by Grants-in-Aid from the Ministry of Education, Culture, Sports, Science and Technology of Japan (HK, HS, MM and YM). This work was also supported by the Science and Technology Incubation Program in Advanced Regions from the funding program 'Creation of Innovation Centers for Advanced Interdisciplinary Research Areas' from the Japan Science and Technology Agency, commissioned by the Ministry of Education, Culture, Sports, Science and Technology (YM). The funders had no role in study design, data collection and analysis, decision to publish, or preparation of the manuscript.

Competing Interests: Kazuaki Matsuoka is an employee of Tokushima Research Center, Taiho Pharmaceutical Co. Ltd (Tokushima, Japan) and Hiroyuki Kitao and Makoto Iimori are staffs of university course financially maintained by donation of Taiho Pharmaceutical Co.Ltd (Department of Molecular Oncology, Kyushu University). However, these do not alter the authors' adherence to all the PLOS ONE policies on sharing data and materials.

* E-mail: hkitao@surg2.med.kyushu-u.ac.jp

Introduction

Hyperthermia is one of the oldest methods used to treat cancer patients. When hyperthermia is combined with other treatments, a significant improvement in the clinical outcome is observed [1]. We have used hyperthermia together with chemoradiotherapy to treat patients with esophageal cancer and rectal cancer with clinical benefit [2,3]. Currently, heat is one of the most potent sensitizers to the action of ionizing radiation (IR) in cells and in human tumors [4], but how heat enhances tumor cytotoxicity is not fully understood.

One possibility is that heat induces DNA damage. DNA degradation was detected in heat-treated Chinese hamster ovary cells by the alkaline elution method [5]. DNA strand scissions were detected as early as 15 minutes in heat-treated HeLa cells in an *in situ* nick translation assay, and the heat-induced DNA scissions were closely correlated with cytotoxicity [6]. These results suggest that DNA single-strand breaks or gaps are induced by heat. Heat also induces the phosphorylation and nuclear foci formation of histone H2AX at Ser139 (γH2AX) [7,8,9]. In many cases, γH2AX nuclear foci are indicators of DNA double-strand breaks (DSBs) [10] and γH2AX plays a critical role in the recruitment of repair factors to sites of DNA damage [11]. Heat-induced γH2AX nuclear foci have been suggested to coincide with heat-induced DNA DSBs, which cause the loss of cell viability [7,8]. Another report showed that DNA DSBs are not associated with heat-induced γH2AX nuclear foci, because the recruitment of DSB repair factors such as 53BP1 and SMC1 was not observed [9].

Heat *per se* induces several steps associated with DNA damage responses (DDR). Heat induces the autophosphorylation of ATM at Ser1981 and activates its kinase activity, but this occurs in the absence of apparent DNA strand breaks [9]. Prior ATM activation by heat may interfere with the normal DDR induced by IR, which is required for the activation of cell cycle checkpoints and chromosomal DNA DSB repair. Indeed, heat perturbs IR-induced DDR mediated by 53BP1 and its downstream targets, which may explain heat radiosensitization [12]. Heat-induced alterations in chromatin structure cause aberrant activation of DDR and reduce

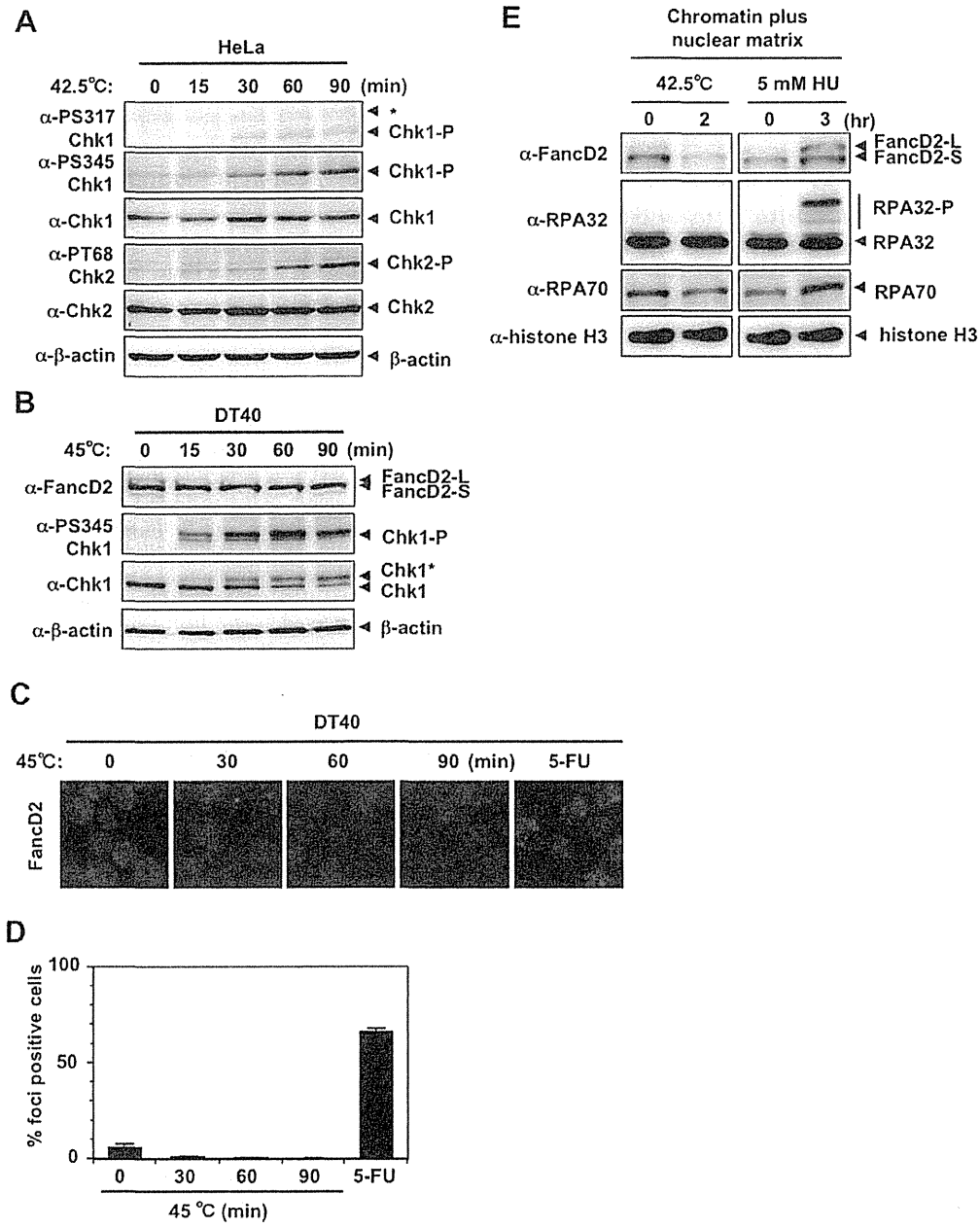

Figure 1. DNA damage response by heat stress. A. Western blot. HeLa cells were cultured at 42.5°C for the indicated time. Non-specific bands were indicated as *. **B.** Western blot. Wild-type DT40 cells were cultured at 45°C for the indicated time. **C.** Nuclear foci of FancD2. Wild-type DT40 cells were cultured at 45°C for the indicated time. Wild-type DT40 cells cultured in the presence of 200 μM 5-FU for 16 hours are shown as a positive control (5-FU) [23]. **D.** The percentage of FancD2 nuclear foci-positive cells in **C** is shown. **E.** Subcellular fractionation of HeLa cells cultured at 42.5°C for 2 hours or at 37°C in the presence of 5 mM hydroxyurea (HU) for 3 hours. Chromatin plus nuclear matrix fraction was isolated as described in Materials and Methods. Ten μg (FancD2, RPA70 and RPA32) or 2 μg (histone H3) of protein were subjected to SDS-PAGE and Western blot.
doi:10.1371/journal.pone.0055361.g001

accessibility of DNA repair machinery to the damage sites of the following IR [4]. Recently, the ATR-Chk1 pathway was shown to be preferentially activated by heat [13]. Selective inhibitors of ATR or Chk1 enhanced heat-induced apoptosis, and their effect was more prominent than selective inhibitors of ATM or Chk2, suggesting the importance of the ATR-Chk1 pathway in protecting cells from heat cytotoxicity. The ATR-Chk1 pathway is activated when replication forks are stalled [14], and various factors, including replication protein A (RPA)-coated single-strand DNA (ssDNA), 5′ ends at primer-template junctions, ATR interacting protein (ATRIP), TopBP1, Claspin, polymerase alpha, Rad9-Rad1-Hus1 (9-1-1) heterotrimeric clamp and Rad17-RFC clamp loader of 9-1-1, are involved in this process [15]. ATR kinase phosphorylates multiple downstream targets other than

Chk1, such as RPA32 [16] and FancI [17,18], which play an important role in S phase checkpoint and Fanconi anemia (FA) pathway activation, respectively. However, it is not known which factors are required for heat-induced activation of the ATR-Chk1 pathway or which downstream targets of ATR kinase are phosphorylated at high temperature.

To understand the mechanism for heat-induced activation of the signaling pathways belonging to ATR-Chk1 and ATM-Chk2 axes, we performed genetic analysis using human HeLa cells and chicken DT40 cells. We found that heat-induced activation of the ATR-Chk1 pathway was largely dependent on Rad9, Rad17, TopBP1 or Claspin, essential factors for activation of ATR-Chk1 pathway at stalled replication forks. Heat-induced activation of the ATR-Chk1 pathway, however, was not associated with FancD2 monoubiquitination, an indicator of FA pathway activation [19], or RPA32 phosphorylation [16], which suggests that heat does not activate all downstream targets of ATR kinase. ATR and ATM kinases contributed to heat tolerance in a non-overlapping manner and simultaneous inhibition of ATR and ATM kinases with caffeine significantly enhanced the cytotoxic effect of hyperthermia. This study revealed the evolutionarily conserved roles of heat-induced activation of DNA damage response.

Results

Heat induction of Chk1 phosphorylation but not of FancD2 monoubiquitination in HeLa cells and chicken DT40 cells

To analyze cellular responses to heat, HeLa and chicken B lymphoma DT40 cells and their mutants were used as model systems. A temperature of 5.5°C above the normal culture temperature (42.5°C for HeLa cells, 45°C for DT40 cells, normal culture temperature for HeLa cells and DT40 cells is 37°C and 39.5°C, respectively) was used to provoke hyperthermia, because this temperature induces cell death via disruption of DNA repair machinery [8].

As reported previously [13], phosphorylation of Chk1 Ser317 and Ser345 and Chk2 Thr68, the primary targets of ATR and ATM kinases, respectively, was induced when HeLa cells were incubated at 42.5°C (Fig. 1A). Chk1 Ser317 and Ser345 phosphorylation was detected as early as 30 minutes after the shift to 42.5°C, whereas phosphorylation of Chk2 Thr68 was detected at 60 minutes (Fig. 1A). In DT40 cells, Chk1 Ser345 phosphorylation was detected as early as 15 minutes after the shift to 45°C (Fig. 1B). In addition, slower migrating forms of Chk1 (indicated as Chk1* in Fig. 1B), indicating its posttranslational modification, were induced with similar kinetics (Fig. 1B). However, monoubiquitination of FancD2 (Fig. 1B) or FancD2 nuclear foci (Fig. 1C and 1D) were not induced by heat in DT40 cells. Furthermore, induction of FancD2 monoubiquitination, RPA32 phosphorylation or RPA70/RPA32 protein accumulation was not detected in the chromatin plus nuclear matrix fraction of heat-treated HeLa cells, while such induction was clearly detected in the chromatin plus nuclear matrix fraction of hydroxyurea (HU)-treated HeLa cells (Fig. 1E). This result suggests that not all downstream events of ATR kinase were induced by heat.

Rad9- and Rad17-deficiency suppressed heat-induced Chk1 Ser345 phosphorylation and enhanced heat cytotoxicity

The 9-1-1 clamp and the Rad17-RFC clamp loader play essential roles in activation of the ATR-Chk1 pathway at stalled replication forks [14,20]. We examined the possible involvement of Rad9 and Rad17 in the heat-induced ATR-Chk1 pathway and heat cytotoxicity. First, we performed immunofluorescent staining of endogenous Rad9 with anti-Rad9 antibody to analyze its subnuclear localization during heat stress. When HeLa cells, transfected with siRNA against *GFP* (as negative control), were pre-extracted by Triton X-100 before fixing with paraformaldehyde, Rad9 signal was detected and visualized as subnuclear foci, whose intensity reduced significantly by siRNA-mediated knockdown of *Rad9* (Fig. S1A). This result indicates that this anti-Rad9 antibody specifically reacted with endogenous Rad9, which accumulates in detergent-resistant subnuclear fraction, possibly chromatin fraction, in normal culture condition. When HeLa cells were incubated at 42.5°C for 30 minutes, similar subnuclear foci of Rad9 were detected, while RPA32 subnuclear foci were not detected (Fig. S1B). In contrast, when cells were treated with 5 mM HU for 3 hours, subnuclear foci of Rad9 were also detected, but some cells were positively stained with RPA32 (Fig. S1B, indicated by white arrowheads). Collectively, these results suggest that Rad9 resided in chromatin fraction even though RPA32 was not actively accumulated in chromatin fraction when cells were exposed to heat stress.

When HeLa cells were treated with siRNA targeting *Rad9* or *Rad17*, heat-induced Chk1 Ser317 and Ser345 phosphorylation was suppressed, while heat-induced Chk2 Thr68 phosphorylation was slightly increased (Fig. 2A). SiRNA-mediated knockdown of *Rad9* or *Rad17* in HeLa cells reduced clonogenic viability at the higher temperature (Fig. 2B). When *Rad9*- or *Rad17*-deficient DT40 cells (*rad9* or *rad17*) [21] were incubated at 45°C, Ser345 phosphorylation of Chk1 was hardly detectable (Fig. 2C). The *rad9* or *rad17* cells also exhibited reduced clonogenic viability at the higher temperature (Fig. 2D). In addition, the cleaved Chk1 peptide was clearly detected when these cells were shifted to 39.5°C after a 1-hour incubation at 45°C (Fig. 2E), while that peptide was hardly detectable when wild-type cells were treated similarly (Fig. S3E). Because this peptide was not detected in the presence of the caspase inhibitor, ZVAD-fmk (Fig. 2E), the peptide must have been produced by caspase-mediated cleavage during apoptosis induced at 45°C [22,23]. Chk1 peptide produced by caspase-mediated cleavage at Asp299 was detected when cells undergo apoptosis and a truncated form of Chk1 mimicking the N-terminal cleavage fragment (residue 1–299) is implicated in enhancing apoptotic reactions [22]. Consistently, the increase in annexin V-positive, PI-negative population was more prominent in heat-treated *rad9* and *rad17* cells than in heat-treated wild-type cells (Fig. 2F). These results indicate that Rad9 and Rad17 were required for activation of the ATR-Chk1 pathway by heat and were involved in the suppression of heat-induced apoptosis, and contributed to the increase in clonogenic viability. Of note, slower migrating forms of Chk1 (Chk1*) were detected in *rad9* and *rad17* cells, suggesting that this posttranslational modification of Chk1 still occurred in the absence of Rad9- or Rad17-dependent ATR activation.

siRNA-mediated knockdown of TopBP1 and Claspin suppressed heat-induced Chk1 Ser345 phosphorylation and enhanced heat cytotoxicity

In the activation of ATR-Chk1 pathway during stalled replication forks, Rad9 and Rad17 cooperate with several essential factors, such as TopBP1 and Claspin [15]. Endogenous TopBP1 was positively stained with anti-TopBP1 antibody by immunofluorescence in detergent pre-extracted HeLa cells, whose intensity decreased significantly by siRNA-mediated knockdown of *TopBP1* (Fig. S1C), confirming the specificity of anti-TopBP1 antibody and its chromatin localization. When HeLa cells were cultured at

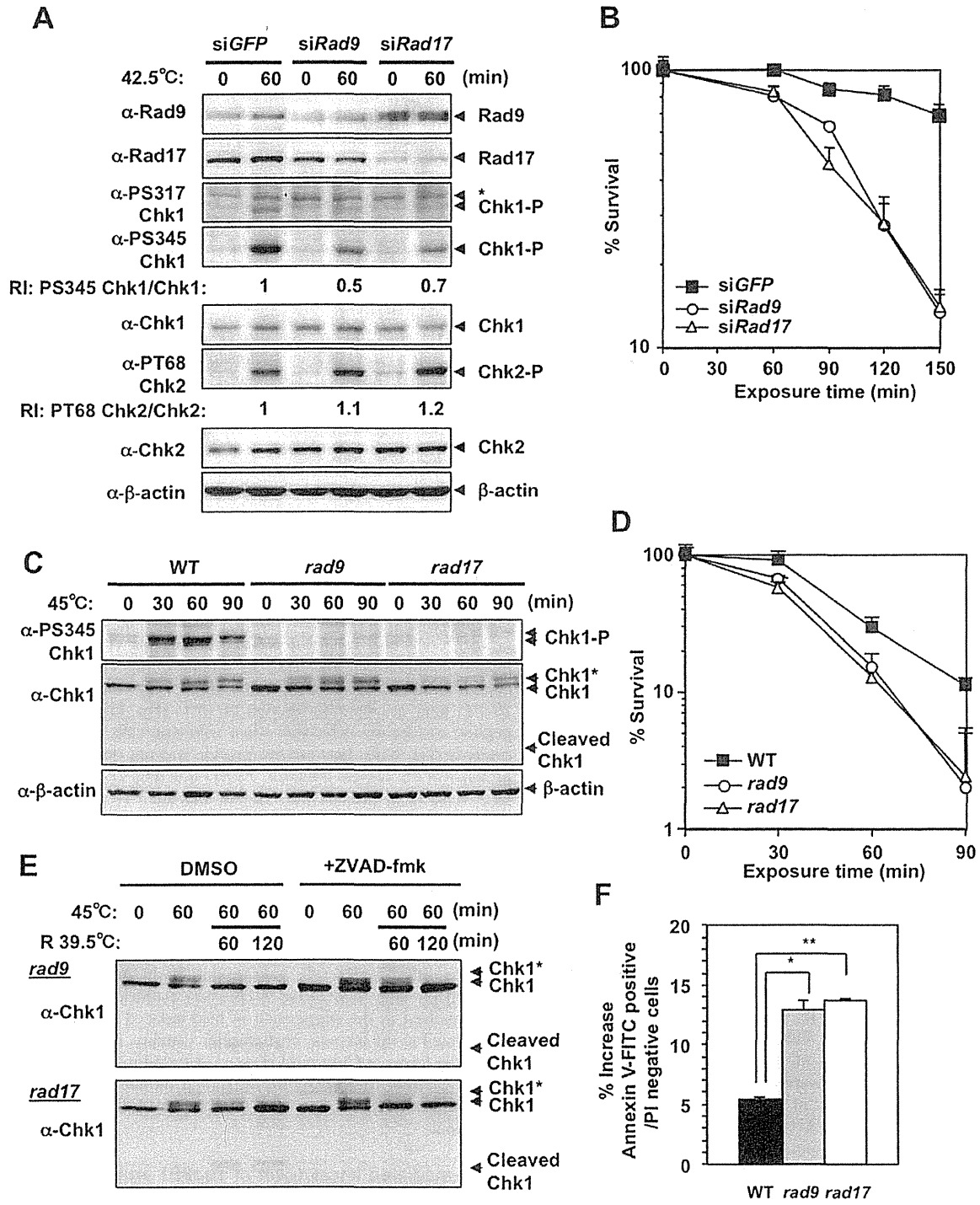

Figure 2. Rad9- or Rad17-deficiency inhibited heat-induced Chk1 phosphorylation at Ser345 and enhanced heat cytotoxicity. A. Western blot. HeLa cells were transfected with siRNA for *GFP*, *Rad9* or *Rad17* and cultured at 42.5°C for 60 minutes. Non-specific bands were indicated as *. RI: relative intensity compared to the sample of *siGFP* and 42.5°C for 60 minutes. **B.** Clonogenic survival. HeLa cells were transfected with siRNA for *GFP*, *Rad9* or *Rad17* and cultured at 42.5°C for the indicated time. **C.** Western blot. Wild-type, *Rad9*- and *Rad17*-deficient DT40 cells (WT, *rad9* or *rad17*) were cultured at 45°C for the indicated time. **D.** Clonogenic survival. WT, *rad9* and *rad17* DT40 cells were cultured at 45°C for the indicated time. **E.** Western blot. The *rad9* and *rad17* DT40 cells were cultured at 45°C for 60 minutes and at 39.5°C for the indicated time in the presence of DMSO or caspase inhibitor (50 μM ZVAD-fmk). **F.** The induction of early apoptotic cells by heat. Early apoptotic cells were detected as annexin V-FITC-positive, propidium iodide (PI)-negative population. WT, *rad9* and *rad17* DT40 cells were cultured at 45°C for 60 minutes and at 39.5°C for 60 minutes, and the increase in early apoptotic cells induced by these treatment is shown. $^{*}p = 0.0016$, $^{**}p = 0.0002$ (Student's *t* test).
doi:10.1371/journal.pone.0055361.g002

42.5°C for 30 min, the detergent-resistant immunofluorescence signal of TopBP1 was similarly detected, while that of RPA32 was not (Fig. S1D). When HeLa cells were cultured in the presence of 5 mM HU for 3 hours (Fig. S1D), the detergent-resistant immunofluorescence signal of TopBP1 was detected, but in this case, some cells were also positively immunostained with RPA32 (Fig. S1D). These results suggest that TopBP1 resided in the chromatin fraction even though RPA32 was not actively accumulated in chromatin fraction when cells were exposed to heat stress.

To test whether TopBP1 and Claspin are also involved in the activation of ATR-Chk1 pathway by heat or heat tolerance, we knocked down *TopBP1* or *Claspin* by siRNA in HeLa cells and analyzed heat-induced phosphorylation of Chk1 and Chk2 or heat cytotoxicity by measuring clonogenic viability. Heat-induced Chk1 Ser345 phosphorylation was significantly suppressed by siRNA-mediated knockdown of TopBP1 (Fig. 3A) or Claspin (Fig. 3C), while heat-induced Chk2 Thr68 phosphorylation was slightly enhanced (Fig. 3A and 3C). Furthermore, siRNA-mediated knockdown of *TopBP1* (Fig. 3B) or *Claspin* (Fig. 3D) decreased clonogenic viability to heat stress significantly. These results indicate that TopBP1 and Claspin were also required for the activation of ATR-Chk1 pathway by heat stress and contributed to the increase in clonogenic viability.

ATM-deficiency results in mild heat sensitivity that is independent of ATR kinase activity

Next, we examined the possible involvement of ATM kinase activity in heat tolerance. In the presence of ATM inhibitor, KU55933, heat-induced Chk2 Thr68 phosphorylation was significantly suppressed, while Chk1 Ser345 phosphorylation was normally induced (Fig. 4A). Clonogenic viability at the higher temperature decreased only slightly in the presence of KU55933 (Fig. 4B). *ATM*-deficient DT40 cells (*atm*) also exhibited slight heat sensitivity (Fig. 4C), while heat-induced Ser345 phosphorylation and slower migrating forms of Chk1 (Chk1*) were detected at normal levels (Fig. S2A). Cleaved Chk1 peptide, which was also suppressed by ZVAD-fmk, was detected when cells were shifted to 39.5°C after a 1-hour incubation at 45°C (Fig. S2B), and the increase in annexin V-positive, PI-negative population was more prominent in heat-treated *atm* cells than in heat-treated wild-type cells (Fig. 4D). To determine whether the ATR-Chk1 and ATM-

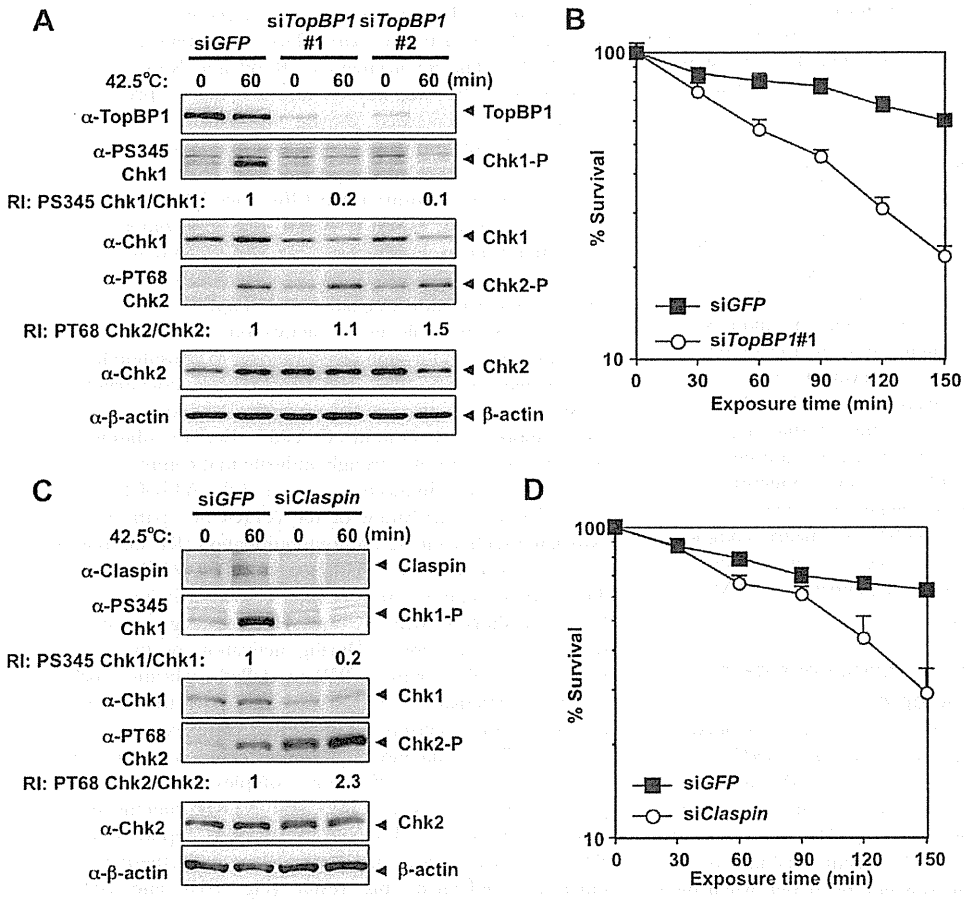

Figure 3. siRNA-mediated knockdown of TopBP1 and Claspin suppressed heat-induced Chk1 Ser345 phosphorylation and enhanced heat cytotoxicity. A. Western blot. HeLa cells were transfected with siRNA for *GFP*, *TopBP1#1* or *TopBP1#2* and cultured at 42.5°C for 60 minutes. RI: relative intensity compared to the sample of si*GFP* and 42.5°C for 60 minutes. **B.** Clonogenic survival. HeLa cells were transfected with siRNA for *GFP or TopBP1#1* and cultured at 42.5°C for the indicated time. **C.** Western blot. HeLa cells were transfected with siRNA for *GFP* or *Claspin* and cultured at 42.5°C for 60 minutes. RI: relative intensity compared to the sample of si*GFP* and 42.5°C for 60 minutes. **D.** Clonogenic survival. HeLa cells were transfected with siRNA for *GFP or Claspin* and cultured at 42.5°C for the indicated time.
doi:10.1371/journal.pone.0055361.g003

Chk2 pathways contribute to heat tolerance in a non-overlapping manner, we analyzed cellular responses and clonogenic viability at the higher temperature in KU55933-treated HeLa cells treated with *ATR* siRNA. SiRNA knockdown of ATR suppressed heat-induced Chk1 Ser345 phosphorylation and slightly enhanced heat-induced Chk2 Thr68 phosphorylation (Fig. 4E), and reduced the clonogenic viability of HeLa cells at the higher temperature (Fig. 4F). KU55933 suppressed the increased phosphorylation of Chk2 Thr68 (Fig. 4E) and increased the heat sensitivity of HeLa cells treated with *ATR* siRNA (Fig. 4F). This result clearly supports the idea that the ATR-Chk1 and ATM-Chk2 pathways contribute to heat tolerance in a non-overlapping manner.

Caffeine suppressed heat-induced phosphorylation of Chk1 Ser345 and Chk2 Thr68 and enhanced heat cytotoxicity

Caffeine is an inhibitor of both ATM and ATR kinase activity [24]. We examined whether caffeine had any effect on heat-induced phosphorylation of Chk1 Ser345 and Chk2 Thr68, and on heat cytotoxicity. In HeLa cells, heat-induced phosphorylation of Chk1 Ser345 and Chk2 Thr68 was significantly suppressed when 12 mM caffeine was added to the medium (Fig. 5A). Clonogenic viability also decreased significantly at the higher temperature in the presence of caffeine (Fig. 5B). Consistently, cells in annexin V-positive, PI-negative population (Fig. 5C) and in subG1 population (Fig. S3A) increased significantly in the presence of caffeine when cells were shifted to 37°C after a 2-hour incubation at 42.5°C. Similarly, in DT40 cells, 2 mM caffeine suppressed heat-induced Chk1 Ser345 phosphorylation (Fig. S3B) and significantly decreased clonogenic viability (Fig, 5D). These effects were observed more clearly as the concentration of caffeine increased (Fig. S3C and S3D). In the presence of 2 mM caffeine, the cleaved Chk1 peptide was detected when cells were shifted to 39.5°C after a 1-hour incubation at 45°C (Fig. S3E). Cells in annexin V-positive, PI-negative population (Fig. 5E) and in subG1 population (Fig. S3F) increased significantly in the presence of caffeine. Even though we were not able to evaluate caffeine's effect on heat-induced Chk2 phosphorylation in DT40 cells due to unavailability of appropriate antibodies, these results suggest that caffeine may have enhanced heat cytotoxicity by suppressing both ATM and ATR kinase activities. Of note, slower migrating forms of Chk1 were still normally detected even in the presence of 8 mM caffeine, while phosphorylation at Ser345 was nearly completely abolished (Fig. S3D). This result also suggests that this post-translational modification of Chk1 was not dependent on ATM/ATR kinase activity.

Caffeine enhanced the heat cytotoxicity of rad9, rad17, and atm cells by increasing apoptosis

To identify the principal target of caffeine in heat cytotoxicity, we performed a clonogenic survival assays for *rad9*, *rad17* and *atm* cells in the presence of 2 mM caffeine. When 2 mM caffeine was added to *atm* cells during heat treatment, heat-induced Chk1 Ser345 phosphorylation was suppressed (Fig. S4A) and clonogenic viability was decreased (Fig. 6A). Clonogenic viability of *rad9* (Fig. 6B) and *rad17* (Fig. 6C) cells was also decreased when these mutant cells were cultured at high temperature in the presence of 2 mM caffeine. A slight increase in the amount of the caspase-cleaved Chk1 peptide was detected when caffeine was added to heat-treated *rad9* (Fig. S4C), *rad17* (Fig. S4D) and *atm* cells (Fig. S4B). Consistently, caffeine induced an increase in the number of cells in annexin V-positive, PI-negative population among *rad9* (Fig. 6E), *rad17* (Fig. 6F) and *atm* (Fig. 6D) cells shifted to 39.5°C after a 1-hour incubation at 45°C. These data further support the idea that heat-induced activation of both ATM and ATR kinases contributes to heat tolerance and that caffeine enhances heat cytotoxicity by inhibiting both ATM and ATR kinases.

Discussion

Hyperthermia exerts pleiotropic effects on proliferating cells and causes cytotoxicity. From the analysis of cellular responses to hyperthermia, we found that the ATR-Chk1 pathway contributes to heat tolerance and that Rad9, Rad17, TopBP1 and Claspin are absolutely required for activation of the ATR-Chk1 pathway at high temperature. ATM-Chk2 pathway was also activated by heat and contributed to heat tolerance mildly but significantly. The ATR-Chk1 and ATM-Chk2 pathways contributed to heat tolerance in a non-overlapping manner and simultaneous inhibition of ATR and ATM kinases significantly enhanced cytotoxicity to hyperthermia.

Rad9 and Rad17 were important for heat-induced activation of the ATR-Chk1 pathway and for heat tolerance (Fig. 2). Rad9 is a component of the 9-1-1 heterotrimeric clamp that binds to 5′ ends of the primer-template junctions containing exposed regions of ssDNA, and Rad17 is an essential component of the 9-1-1-clamp loader complex. Both of these factors are required for activation of the ATR-Chk1 pathway, particularly when replication forks are stalled [20]. The involvement of Rad9 and Rad17 in the heat response suggests that ssDNA and 5′ ends of primer-template junctions are generated during hyperthermia. This idea is supported by our previous study using the *in situ* nick translation method, which revealed the presence of DNA strand scissions in HeLa cells upon exposure to heat [6]. Such DNA structures might be formed when DNA synthesis ceases incompletely during replication process. Furthermore, we also found that heat-induced Chk1 Ser345 phosphorylation was significantly suppressed by siRNA-mediated downregulation of TopBP1 (Fig. 3A), which plays an essential role in the activation of ATR kinase via its activation domain through direct binding to phosphorylated Rad9 at damaged DNA [25]. SiRNA-mediated downregulation of Claspin, which is an essential upstream regulator of Chk1 [26], also suppressed heat-induced Chk1 Ser345 phosphorylation (Fig. 3C). These results strongly indicate that common mechanism is involved in heat-induced activation of the ATR-Chk1 pathway.

Heat-induced activation of the ATR-Chk1 pathway was not associated with FancD2 monoubiquitination, RPA32 phosphorylation or chromatin accumulation of RPA70/RPA32 (Fig. 1E). This is quite different from cellular responses induced by HU or DNA crosslinkers, which causes DNA damage associated with stalled replication forks. During activation of the ATR-Chk1 pathway by DNA damage (IR) or stalled replication forks (HU, ultraviolet irradiation), ssDNA is coated by the trimeric RPA complex, which recruits ATR-ATRIP complex to sites of DNA damage [27]. For the induction of FancD2 monoubiquitination, in addition to functional FA core complex [19], ATR-mediated phosphorylation of FancI [17] and ATRIP binding to RPA70 [28], are required. However, a previous report showed that RPA32 nuclear foci do not form during hyperthermia [13]. We ourselves confirmed this result (Fig. S1B and S1D). The recruitment of RPA32 to ssDNA might be inhibited through its direct sequestering by nucleolin, which relocalizes from the nucleolus to nucleoplasm and increases its binding to RPA32 by heat stress [29]. Even though ATRIP is supposed to recognize RPA-ssDNA complex to sense DNA damage [27], other report shows that RPA32 downregulation do not suppress HU-induced Chk1 Ser345 phosphorylation [30]. In addition, Chk1 Ser345

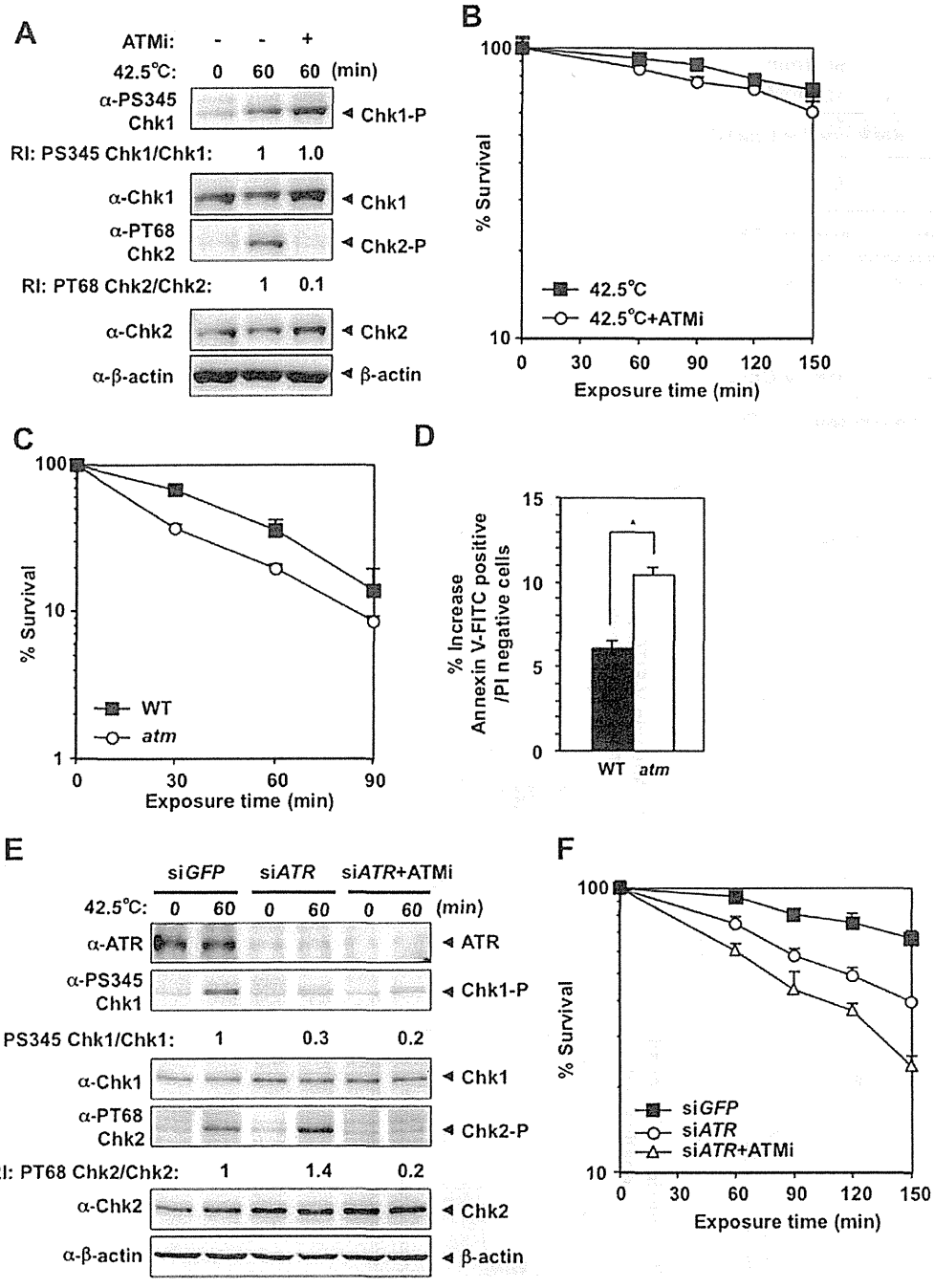

Figure 4. ATM-deficiency inhibited heat-induced Chk2 Thr68 phosphorylation and enhanced heat cytotoxicity. A. Western blot. HeLa cells were cultured at 42.5°C for 60 minutes in the presence or absence of the ATM inhibitor KU55933 (ATMi). RI: relative intensity compared to the sample of ATMi (−) and 42.5°C for 60 minutes. **B.** Clonogenic survival. HeLa cells were cultured at 42.5°C for the indicated time in the presence or absence of ATMi. **C.** Clonogenic survival. Wild-type and *Atm*-deficient DT40 cells (WT or *atm*) were cultured at 45°C for the indicated time. **D.** Apoptosis. WT and *atm* DT40 cells were cultured at 45°C for 60 minutes and at 39.5°C for 60 minutes, and the increase in the number of early apoptotic cells induced by these treatments is shown. $*p = 0.0131$ (Student's *t* test). **E.** Western blot. HeLa cells transfected with siRNA for *GFP* or *ATR* (in the presence or absence of ATMi) were cultured at 42.5°C for 60 minutes. RI: relative intensity compared to the sample of si*GFP* and 42.5°C for 60 minutes. **F.** Clonogenic survival. HeLa cells transfected with siRNA for *GFP* or *ATR* (in the presence or absence of ATMi) were cultured at 42.5°C for the indicated time.

doi:10.1371/journal.pone.0055361.g004

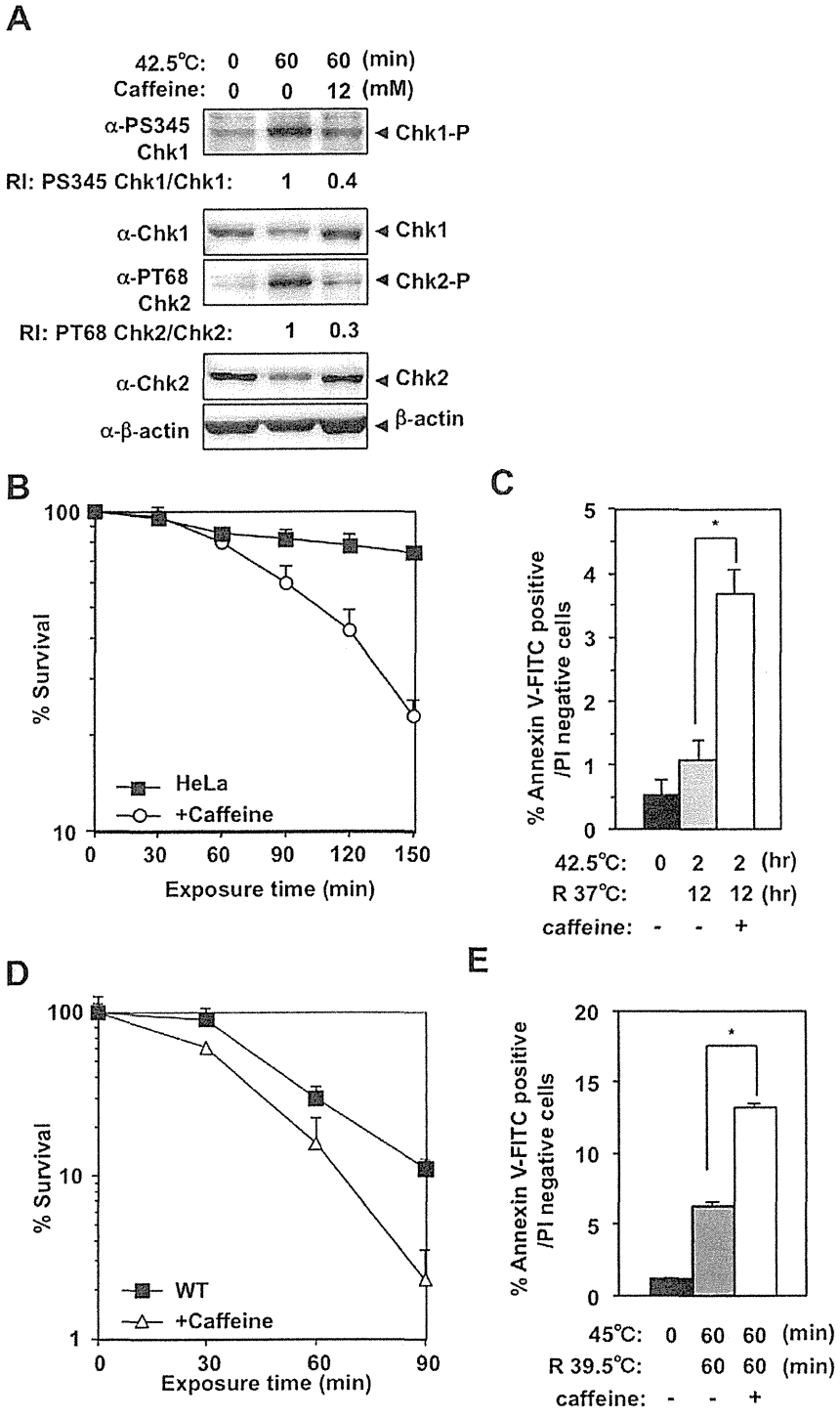

Figure 5. Caffeine suppressed heat-induced phosphorylation at Chk1 Ser345 and Chk2 Thr68 and enhanced heat cytotoxicity. A. Western blot. HeLa cells were cultured at 42.5°C for 1 hour in the presence or absence of 12 mM caffeine. RI: relative intensity compared to the sample of 42.5°C for 60 minutes. **B.** Clonogenic survival of heat-treated HeLa cells in the presence or absence of 12 mM caffeine. **C.** Apoptosis. HeLa cells were cultured at 42.5°C for 2 hours and at 37°C for 12 hours in the presence or absence of 12 mM caffeine. *$p = 0.0019$ (Student's t test). **D.** Clonogenic survival of WT DT40 cells cultured at 45°C for the indicated time in the presence or absence of 2 mM caffeine. **E.** Apoptosis. WT DT40 cells were cultured at 45°C for 60 minutes and at 39.5°C for 60 minutes in the presence or absence of 2 mM caffeine. *$p = 0.0014$ (Student's t test).
doi:10.1371/journal.pone.0055361.g005

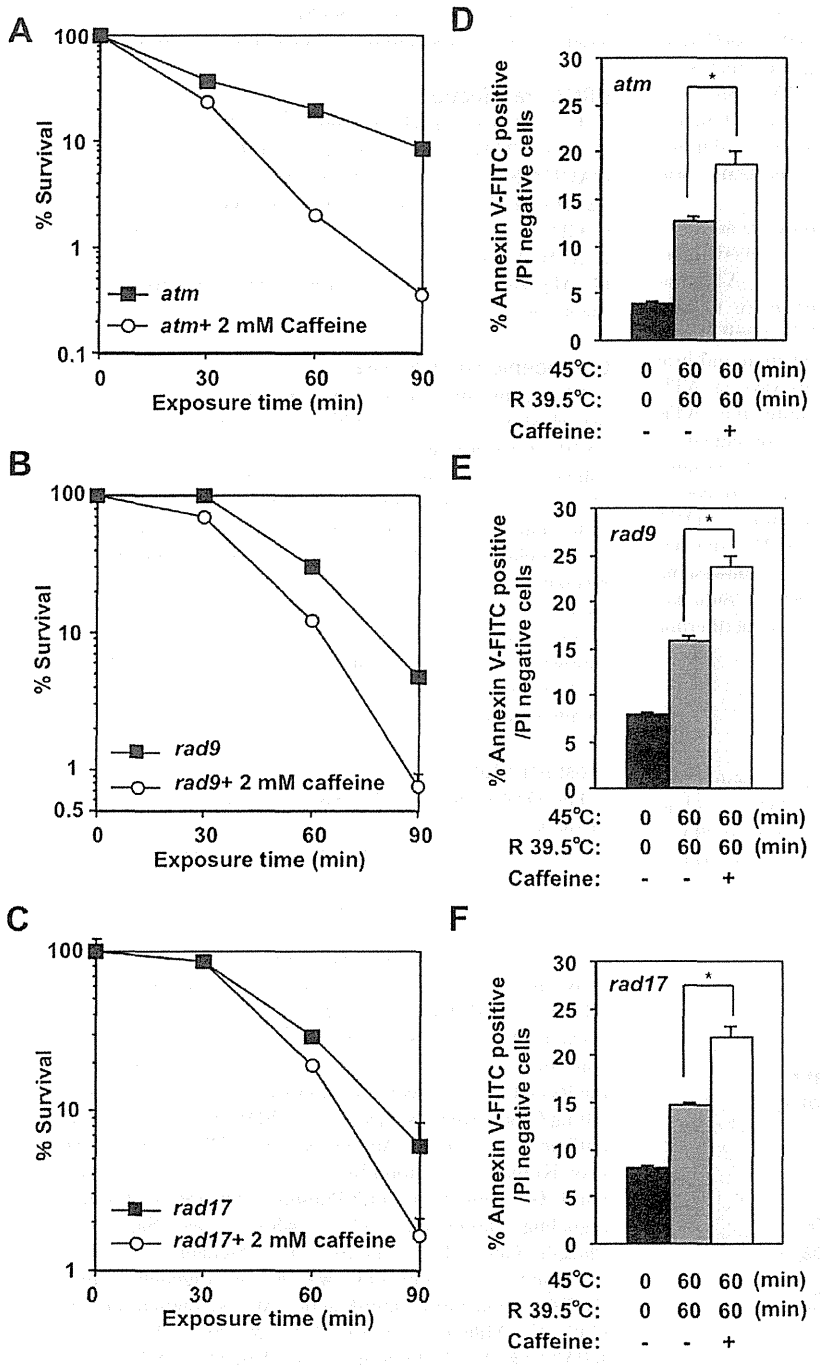

Figure 6. Caffeine enhanced the heat cytotoxicity of *rad9, rad17* or *atm* DT40 cells. A–C. Clonogenic survival. *atm* (**A**), *rad9* (**B**) and *rad17* (**C**) DT40 cells were cultured at 45°C for the indicated time in the presence or absence of 2 mM caffeine. **D–F.** Apoptosis. *atm* (**D**), *rad9* (**E**) and *rad17* (**F**) DT40 cells were cultured at 45°C for 60 minutes and at 39.5°C for 60 minutes in the presence or absence of 2 mM caffeine. (**D**) $*p = 0.0012$, (**E**) $*p = 0.0057$, (**F**) $*p = 0.0084$ (Student's *t* test).
doi:10.1371/journal.pone.0055361.g006

phosphorylation occurs in the absence of RPA32 through the direct binding of ATRIP to DNA in *Xenopus* system [31]. The activation of ATR kinase and phosphorylation of Chk1 Ser345 could occur in the absence of functional RPA-ssDNA complex at damage site during hyperthermia, but the downstream events, such as RPA32 phosphorylation or FancD2 monoubiquitination, might be perturbed because of its absence.

The heat-induced emergence of slow migrating forms of Chk1 in DT40 cells (Fig. 1B) indicated that heat induced posttranslational modification(s) of Chk1. The slow migrating forms of Chk1 were also detected even in heat-treated *rad9*, *rad17* (Fig. 2C) and

atm cells (Fig. S2A). These forms were still detectable even in caffeine-treated wild type (Fig. S3B), *rad9* (Fig. S4C), *rad17* (Fig. S4D) and *atm* cells (Fig. S4B). This result suggests that such posttranslational modifications of Chk1 occur in ATM- and ATR-independent manner. This modification may alter Chk1 function or activity. We are currently interested in this possibility and trying to clarify its possible role in cellular response to heat and heat tolerance.

Both the ATR-Chk1 and ATM-Chk2 pathways were activated by heat and contributed to heat tolerance in a non-overlapping manner (Fig. 7). Consistent with a previous report [13], ATR was preferentially activated by heat and contributed more to heat tolerance than ATM. Furthermore, Rad9, Rad17, TopBP1 and Claspin were required for heat-induced ATR activation and heat tolerance. Interestingly, not all downstream pathways of ATR kinase were activated by heat treatment, indicating that ATR activation by hyperthermia has distinct biological consequences. Finally, inhibition of ATM and ATR kinase activity at the same time by caffeine was effective way to enhance heat cytotoxicity, which could have clinical implication. The activation of DNA damage signaling by heat may compromise normal DNA damage responses. Our findings may provide some clues to understand why hyperthermia potentiates the cytotoxic effects of radiation therapy and chemotherapy and help us to improve hyperthermia therapeutic strategy.

Materials and Methods

Cell lines, cell culture and reagents

HeLa cells were cultured at 37°C in DMEM supplemented with 10% FBS. The chicken B lymphoma cell line DT40 and its mutants (*rad9* [21], *rad17* [21] or *atm* [32]) were cultured at 39.5°C in RPMI1640 supplemented with 10% fetal bovine serum (FBS), 1% chicken serum, penicillin-streptomycin, L-glutamine and β-mercaptoethanol, as described previously [33]. UCN-01 and KU55933 were purchased from Sigma, caffeine was from Nacalai Tesque, and caspase inhibitor ZVAD-fmk was from MBL.

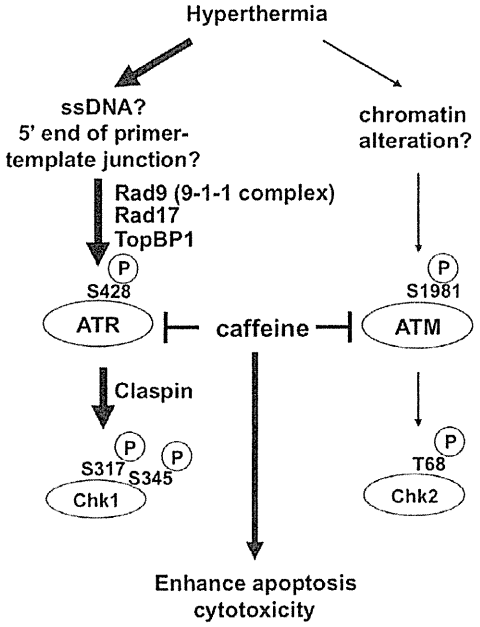

Figure 7. Model of cellular response to heat stress. See text for details.
doi:10.1371/journal.pone.0055361.g007

siRNA transfection

The following siRNAs were used: *Rad9:* 5′-GCAAACUUGAAUCUUAGCA-3′; *Rad17:* 5′-CAAGUACAAGAGUGGAUUA-3′; *ATR:* 5′-CCUCCGUGAUGUUGCUUGA-3′ [34]. *TopBP1*#1: 5′-CUCACCUUAUUGCAGGAGA-3′; *TopBP1*#2: 5′-CUCACCUUAUUGCAGGAGA-3′ [35]; *Claspin:* 5′-GCACAUACAUGAUAAAGAA-3′, *GFP:* 5′-UCUUAAUCGCGUAUAAGGC-3′. siRNAs were transfected using RNAiMax (Invitrogen).

Clonogenic survival assay

Clonogenic survival assay was performed with DT40 cells as described previously [36] with the following modifications. Briefly, 1×10^4 cells were suspended in 1 ml culture media with or without caffeine in an eppendorf tube. After 10 minutes preincubation at 39.5°C, the cells were exposed to heat by placing each tube in a water bath at 45°C. After incubation for the indicated times, 1×10^2 cells were plated on methylcellulose-containing media, and incubated for 1–2 weeks at 39.5°C. Emerging colonies were counted. For the HeLa cell, 2×10^2 cells were inoculated into 60 mm^2 plates and incubated at 37°C for 24 hours. Cells were exposed to 42.5°C for the indicated times and incubated at 37°C for 10 days. Emerging colonies were stained with crystal violet and counted. All experiments were done in triplicate.

Western blot analysis

For DT40 cells, 5×10^5 cells were suspended in 1 ml culture media in an eppendorf tube and incubated at 45°C in water bath. After incubation for the indicated times, cells were collected by centrifugation and re-suspended in 1×SDS sample buffer. For HeLa cells, 5×10^5 cells were incubated at 42.5°C for the indicated times and harvested. Collected cells were lysed in RIPA buffer (1.0% NP40; 50 mM Tris HCl, pH 8.0; 150 mM NaCl; 0.5% deoxycholate; 0.1% SDS; 2 mM phenylmethylsulfonyl fluoride (PMSF); 2 mM NaF and 2 mM Na_3VO_4 with protease inhibitor cocktail (Nacalai Tesque)) for 30 minutes at 4°C. The protein concentration of extracts and cleared lysates were determined by the RC DC Protein Assay Kit (Bio-Rad). Equal amounts of protein (10 μg/lane) were subjected to SDS-PAGE. The following antibodies were used; Anti-chicken FancD2 (kindly provided by Prof. Komatsu, Radiation Biology Center, Kyoto University), anti-Chk1 (G4, Santa Cruz), anti-Phospho-Chk1 (Ser345) (#2341, Cell Signaling), anti-Chk2 (1C12) (#3440, Cell Signaling), anti-Phospho-Chk2 (Thr68) (#2661, Cell Signaling), anti-Rad9 (M-389, Santa Cruz), anti-ATR (#2790, Cell Signaling), anti-Rad17 (H-300, Santa Cruz), anti-β-actin (AC-74, Sigma), anti-TopBP1 (AB3245, Millipore), anti-RPA70 (#2589-1, Epitomics), anti-RPA32 (#2461-1, Epitomics), anti-FancD2 (LS-B493, LS Bio), anti-Claspin (A300-266A, Bethyl) and anti-histone H3 (H9289, Sigma). Relative intensity of phosphorylation level of Chk1 (Ser345) and Chk2 (Thr68) were determined by band intensity measured by Image J software (NIH).

Cell cycle analysis

Cells were exposed to heat for the indicated times and fixed with 70% ethanol immediately. DNA contents were analyzed using fixed cells treated with propidium iodide (PI) and RNaseA. The samples were analyzed using FACSCalibur (BD Biosciences) and % of subG1 population (<2N) was calculated.

Detection of early apoptotic cells using Annexin V-FITC

Early apoptotic cells were detected using an Annexin V–FITC apoptosis detection kit (Sigma) as described previously [23]. Briefly, 5×10^5 cells were resuspended in 0.5 ml of 1× binding buffer (10 mM HEPES/NaOH, pH 7.5, 140 mM NaCl, 2.5 mM $CaCl_2$) and stained with 0.5 μg/ml of the annexin V–FITC conjugate and 2 μg/ml PI for 10 minutes at room temperature before FACS analysis. Annexin V–FITC-positive, PI-negative cells were counted as early apoptotic cells. Experiments were done in triplicate.

Isolation of chromatin plus nuclear matrix fraction from HeLa cells

Subcellular fractionation was done as described previously [37]. Briefly, cells were resuspended (4×10^7 cells/ml) in buffer A (10 mM HEPES [pH 7.9], 10 mM KCl, 1.5 mM $MgCl_2$, 0.34 M Sucrose, 10% Glycerol, 1 mM DTT, 0.1 mM PMSF with protease inhibitor cocktail). 0.1% Triton X-100 was added and the cells were incubated on ice for 5 minutes. Nuclei were collected in pellet by low-speed centrifugation (4 minutes, 1,300× *g*, 4°C). Nuclei were washed once in buffer A, and then lysed in buffer B (3 mM EDTA, 0.2 mM EGTA, 1 mM DTT, 0.1 mM PMSF with protease inhibitor cocktail). Insoluble chromatin plus nuclear matrix fraction was collected in pellet by centrifugation (4 minutes, 1,700× *g*, 4°C) and washed once in buffer B. Final pellet was resuspended in 1xSDS buffer and sonicated. Protein concentration was determined by the RC DC Protein Assay Kit and appropriate amount of protein was subjected to SDS-PAGE and Western blot.

Fluorescence immunostaining

Immunostaining was done as described previously [38]. Cells were grown as monolayers on glass coverslips and pre-extracted in Buffer 1 (1% Triton X-100, 10 mM HEPES pH 7.4, 10 mM NaCl, 3 mM $MgCl_2$) for 5 minutes at 4°C. Cells were then fixed in 4% paraformaldehyde for 10 minutes at 4°C and permeabilized further in Buffer 2 (0.5% Triton X-100, 20 mM HEPES pH 7.4, 50 mM NaCl, 3 mM $MgCl_2$, 300 mM sucrose) for 5 minutes at 4°C. To detect endogenous Rad9, RPA32 and TopBP1, the following primary antibodies were used; Rad9 (IHC-00376, Bethyl, 1:50 dilution), RPA32 (GTX16855, Genetex, 1:50 dilution) and TopBP1 (AB3245, Millipore, 1:100 dilution). Cells were stained with an Alexa488- or Alexa594-conjugated secondary antibody (Invitrogen) and the nuclei were counterstained with 4′,6-diamino-2-phenylindole (DAPI). All images were captured using a BIOREVO BZ-9000 fluorescence microscope (Keyence).

Supporting Information

Figure S1 Chromatin localization of Rad9 and TopBP1 in HeLa cells. A. Immunofluorescence staining with anti-Rad9 antibody. HeLa cells were treated with siRNA of *GFP* or *Rad9*, pre-extracted by detergent and immunostained with anti-Rad9 antibody. Nuclei were counterstained with 4′,6-diamino-2-phenylindole (DAPI). White arrowhead indicates a cell in M phase. **B.** Coimmunostaining of Rad9 and RPA32. HeLa cells were cultured at 37°C, 42.5°C or in the presence of 5 mM hydroxyurea (HU), pre-extracted by detergent and coimmunostained with Rad9 and RPA32 antibodies. Nuclei were counterstained with DAPI. White arrowheads indicate RPA32-positive cells. **C.** Immunofluorescence staining with anti-TopBP1 antibody. HeLa cells were treated with siRNA of *GFP* or *TopBP1*, pre-extracted by detergent and immunostained with anti-TopBP1 antibody. Nuclei were counterstained with DAPI. **D.** Coimmunostaining of TopBP1 and RPA32. White arrowheads indicate RPA32-positive cells.
(TIFF)

Figure S2 Cellular response to heat in *ATM*-deficient DT40 cells. A. Western blot. Wild-type (WT) and *ATM*-deficient (*atm*) DT40 cells were cultured at 45°C for the indicated time. RI: relative intensity compared to the sample of 45°C for 15 minutes in WT DT40 cells. **B.** Disappearance of the cleaved Chk1 peptide following treatment with the caspase inhibitor, ZVAD-fmk. *atm* cells were cultured at 45°C for 60 minutes and at 39.5°C for the indicated time in the presence or absence of 50 μM ZVAD-fmk.
(TIFF)

Figure S3 Caffeine enhanced heat cytotoxicity. A. SubG1 population. HeLa cells were cultured at 42.5°C for 2 hours and at 37°C for 12 or 24 hours in the presence or absence of 12 mM caffeine. $*p=0.0016$, $**p=0.0002$ (Student's *t* test). **B.** Western blot. Wild-type DT40 cells (WT) were cultured at 45°C for the indicated time in the presence or absence of 2 mM caffeine. **C.** Clonogenic survival. WT DT40 cells were cultured at 45°C for the indicated time in the presence of various concentration of caffeine. **D.** Western blot. WT DT40 cells were cultured at 45°C for 30 minutes in the presence of various concentration of caffeine. RI: relative intensity compared to the sample of 45°C for 30 minutes without caffeine in WT DT40 cells. **E.** Western blot. WT DT40 cells were cultured at 45°C for 60 minutes and at 39.5°C for the indicated time in the presence or absence of 2 mM caffeine. **F.** SubG1 population. WT DT40 cells were cultured at 45°C for 60 minutes and at 39.5°C for 60 minutes in the presence or absence of 2 mM caffeine. $*p=0.0069$ (Student's *t* test).
(TIFF)

Figure S4 Cellular response to heat in the presence of caffeine in mutant DT40 cells. A. Western blot. *ATM*-deficient DT40 cells (*atm*) were cultured at 45°C for the indicated time in the presence or absence of 2 mM caffeine. **B–D.** Western blot. *atm* (**B**), *rad9* (**C**) and *rad17* (**D**) DT40 cells were cultured at 45°C for 60 minutes and at 39.5°C for the indicated time in the presence or absence of 2 mM caffeine. The percentage of cleaved Chk1 peptide per total.
(TIFF)

Acknowledgments

We thank Dr. Ken-ichi Yamamoto (Cancer Research Institute, Kanazawa University, Japan) for providing *Rad9*- [21], *Rad17*- [21] and *Atm*- [32] deficient DT40 cells, Dr. Kenshi Komatsu (Radiation Biology Center, Kyoto University, Japan) for providing antibody and Dr. Minoru Takata (Radiation Biology Center, Kyoto University, Japan) for critical reading of the manuscript. We also thank Dr. Yoshihiko Fujinaka, Dr. Ryota Nakanishi, Dr. Nami Yamashita, Ms. Naoko Katakura and Ms. Mariko Shimokawa for expert technical assistance and the Research Support Center, Graduate School of Medical Sciences, Kyushu University for technical support.

Author Contributions

N/A. Conceived and designed the experiments: HK MM YM. Performed the experiments: MT HK KM. Analyzed the data: MT HK MI KM SK HS EO MM YM. Contributed reagents/materials/analysis tools: HK MI KM YM. Wrote the paper: MT HK MM YM.

References

1. Horsman MR, Overgaard J (2007) Hyperthermia: a potent enhancer of radiotherapy. Clin Oncol (R Coll Radiol) 19: 418–426.
2. Ohno S, Tomoda M, Tomisaki S, Kitamura K, Mori M, et al. (1997) Improved surgical results after combining preoperative hyperthermia with chemotherapy and radiotherapy for patients with carcinoma of the rectum. Dis Colon Rectum 40: 401–406.
3. Morita M, Kuwano H, Araki K, Egashira A, Kawaguchi H, et al. (2001) Prognostic significance of lymphocyte infiltration following preoperative chemoradiotherapy and hyperthermia for esophageal cancer. Int J Radiat Oncol Biol Phys 49: 1259–1266.
4. Kampinga HH, Dikomey E (2001) Hyperthermic radiosensitization: mode of action and clinical relevance. Int J Radiat Biol 77: 399–408.
5. Warters RL, Henle KJ (1982) DNA degradation in chinese hamster ovary cells after exposure to hyperthermia. Cancer Res 42: 4427–4432.
6. Anai H, Maehara Y, Sugimachi K (1988) In situ nick translation method reveals DNA strand scission in HeLa cells following heat treatment. Cancer Lett 40: 33–38.
7. Kaneko H, Igarashi K, Kataoka K, Miura M (2005) Heat shock induces phosphorylation of histone H2AX in mammalian cells. Biochem Biophys Res Commun 328: 1101–1106.
8. Takahashi A, Matsumoto H, Nagayama K, Kitano M, Hirose S, et al. (2004) Evidence for the involvement of double-strand breaks in heat-induced cell killing. Cancer Res 64: 8839–8845.
9. Hunt CR, Pandita RK, Laszlo A, Higashikubo R, Agarwal M, et al. (2007) Hyperthermia activates a subset of ataxia-telangiectasia mutated effectors independent of DNA strand breaks and heat shock protein 70 status. Cancer Res 67: 3010–3017.
10. Rogakou EP, Pilch DR, Orr AH, Ivanova VS, Bonner WM (1998) DNA double-stranded breaks induce histone H2AX phosphorylation on serine 139. J Biol Chem 273: 5858–5868.
11. Paull TT, Rogakou EP, Yamazaki V, Kirchgessner CU, Gellert M, et al. (2000) A critical role for histone H2AX in recruitment of repair factors to nuclear foci after DNA damage. Curr Biol 10: 886–895.
12. Laszlo A, Fleischer I (2009) Heat-induced perturbations of DNA damage signaling pathways are modulated by molecular chaperones. Cancer Res 69: 2042–2049.
13. Furusawa Y, Iizumi T, Fujiwara Y, Zhao QL, Tabuchi Y, et al. (2012) Inhibition of checkpoint kinase 1 abrogates G2/M checkpoint activation and promotes apoptosis under heat stress. Apoptosis 17: 102–112.
14. Cimprich KA, Cortez D (2008) ATR: an essential regulator of genome integrity. Nat Rev Mol Cell Biol 9: 616–627.
15. Yan S, Michael WM (2009) TopBP1 and DNA polymerase alpha-mediated recruitment of the 9-1-1 complex to stalled replication forks: implications for a replication restart-based mechanism for ATR checkpoint activation. Cell Cycle 8: 2877–2884.
16. Olson E, Nievera CJ, Klimovich V, Fanning E, Wu X (2006) RPA2 is a direct downstream target for ATR to regulate the S-phase checkpoint. J Biol Chem 281: 39517–39533.
17. Ishiai M, Kitao H, Smogorzewska A, Tomida J, Kinomura A, et al. (2008) FANCI phosphorylation functions as a molecular switch to turn on the Fanconi anemia pathway. Nat Struct Mol Biol 15: 1138–1146.
18. Kitao H, Takata M (2011) Fanconi anemia: a disorder defective in the DNA damage response. Int J Hematol 93: 417–424.
19. Wang W (2007) Emergence of a DNA-damage response network consisting of Fanconi anaemia and BRCA proteins. Nat Rev Genet 8: 735–748.
20. Parrilla-Castellar ER, Arlander SJ, Karnitz L (2004) Dial 9-1-1 for DNA damage: the Rad9-Hus1-Rad1 (9-1-1) clamp complex. DNA Repair (Amst) 3: 1009–1014.
21. Kobayashi M, Hirano A, Kumano T, Xiang SL, Mihara K, et al. (2004) Critical role for chicken Rad17 and Rad9 in the cellular response to DNA damage and stalled DNA replication. Genes Cells 9: 291–303.
22. Matsuura K, Wakasugi M, Yamashita K, Matsunaga T (2008) Cleavage-mediated activation of Chk1 during apoptosis. J Biol Chem 283: 25485–25491.
23. Fujinaka Y, Matsuoka K, Iimori M, Tuul M, Sakasai R, et al. (2012) ATR-Chk1 signaling pathway and homologous recombinational repair protect cells from 5-fluorouracil cytotoxicity. DNA Repair (Amst) 11: 247–258.
24. Sarkaria JN, Busby EC, Tibbetts RS, Roos P, Taya Y, et al. (1999) Inhibition of ATM and ATR kinase activities by the radiosensitizing agent, caffeine. Cancer Res 59: 4375–4382.
25. Lee J, Kumagai A, Dunphy WG (2007) The Rad9-Hus1-Rad1 checkpoint clamp regulates interaction of TopBP1 with ATR. J Biol Chem 282: 28036–28044.
26. Kumagai A, Dunphy WG (2000) Claspin, a novel protein required for the activation of Chk1 during a DNA replication checkpoint response in Xenopus egg extracts. Mol Cell 6: 839–849.
27. Zou L, Elledge SJ (2003) Sensing DNA damage through ATRIP recognition of RPA-ssDNA complexes. Science 300: 1542–1548.
28. Shigechi T, Tomida J, Sato K, Kobayashi M, Eykelenboom JK, et al. (2012) ATR-ATRIP kinase complex triggers activation of the Fanconi anemia DNA repair pathway. Cancer Res 72: 1149–1156.
29. Wang Y, Guan J, Wang H, Leeper D, Iliakis G (2001) Regulation of dna replication after heat shock by replication protein a-nucleolin interactions. J Biol Chem 276: 20579–20588.
30. Sleeth KM, Sorensen CS, Issaeva N, Dziegielewski J, Bartek J, et al. (2007) RPA mediates recombination repair during replication stress and is displaced from DNA by checkpoint signalling in human cells. J Mol Biol 373: 38–47.
31. Kim SM, Kumagai A, Lee J, Dunphy WG (2005) Phosphorylation of Chk1 by ATM- and Rad3-related (ATR) in Xenopus egg extracts requires binding of ATRIP to ATR but not the stable DNA-binding or coiled-coil domains of ATRIP. J Biol Chem 280: 38355–38364.
32. Takao N, Kato H, Mori R, Morrison C, Sonada E, et al. (1999) Disruption of ATM in p53-null cells causes multiple functional abnormalities in cellular response to ionizing radiation. Oncogene 18: 7002–7009.
33. Yamamoto K, Hirano S, Ishiai M, Morishima K, Kitao H, et al. (2005) Fanconi anemia protein FANCD2 promotes immunoglobulin gene conversion and DNA repair through a mechanism related to homologous recombination. Mol Cell Biol 25: 34–43.
34. Yang XH, Shiotani B, Classon M, Zou L (2008) Chk1 and Claspin potentiate PCNA ubiquitination. Genes Dev 22: 1147–1152.
35. Kim JE, McAvoy SA, Smith DI, Chen J (2005) Human TopBP1 ensures genome integrity during normal S phase. Mol Cell Biol 25: 10907–10915.
36. Yamamoto K, Ishiai M, Matsushita N, Arakawa H, Lamerdin JE, et al. (2003) Fanconi anemia FANCG protein in mitigating radiation- and enzyme-induced DNA double-strand breaks by homologous recombination in vertebrate cells. Mol Cell Biol 23: 5421–5430.
37. Mendez J, Stillman B (2000) Chromatin association of human origin recognition complex, cdc6, and minichromosome maintenance proteins during the cell cycle: assembly of prereplication complexes in late mitosis. Mol Cell Biol 20: 8602–8612.
38. Medhurst AL, Warmerdam DO, Akerman I, Verwayen EH, Kanaar R, et al. (2008) ATR and Rad17 collaborate in modulating Rad9 localisation at sites of DNA damage. J Cell Sci 121: 3933–3940.

Cancer Medicine

Open Access

ORIGINAL RESEARCH

Differential impact of the expression of the androgen receptor by age in estrogen receptor–positive breast cancer

Eriko Tokunaga[1,2], Yuichi Hisamatsu[1], Kenji Taketani[1], Nami Yamashita[1], Sayuri Akiyoshi[1], Satoko Okada[1], Kimihiro Tanaka[1], Hiroshi Saeki[1], Eiji Oki[1], Shinichi Aishima[3], Yoshinao Oda[3], Masaru Morita[1] & Yoshihiko Maehara[1]

[1]Department of Surgery and Science, Graduate School of Medical Sciences, Kyushu University, Fukuoka, Japan
[2]Department of Comprehensive Clinical Oncology, Graduate School of Medical Sciences, Kyushu University, Fukuoka, Japan
[3]Department of Anatomic Pathology, Pathological Sciences, Graduate School of Medical Sciences, Kyushu University, Fukuoka, Japan

Keywords
Androgen receptor, breast cancer, estrogen receptor, phenotype, postmenopausal

Correspondence
Eriko Tokunaga, Department of Surgery and Science, Graduate School of Medical Sciences, Kyushu University, 3-1-1 Maidashi, Higashi-ku, Fukuoka 812-8582, Japan.
Tel: +81-92-642-5466; Fax: +81-92-642-5482;
E-mail: eriko@surg2.med.kyushu-u.ac.jp

Funding Information
This study was supported by grants from the Ministry of Education, Culture, Sports Science, and Technology of Japan (Grant No. 23591896).

Received: 20 May 2013; Revised: 4 August 2013; Accepted: 5 August 2013

Cancer Medicine 2013; 2(6): 763–773

doi: 10.1002/cam4.138

Abstract

We evaluated the expression of the androgen receptor (AR) to determine its significance in breast cancer. AR expression levels were analyzed in 250 invasive breast cancers by immunohistochemistry and any association with the clinicopathological features was evaluated. AR expression was higher in estrogen receptor (ER)-positive cases than in ER-negative cases ($P < 0.0001$). AR expression was associated with ER level, and it increased with age in ER-positive cases. The cut-off value was determined to be 75% (*Cancer Res.* 2009;69:6131–6140), and AR expression was considered to be high in 155 (62%) cases. High AR expression significantly correlated with lower nuclear grade ($P < 0.0001$), ER and progesterone receptor (PR) positivity ($P < 0.0001$ and $P = 0.0022$), HER2 negativity ($P = 0.0113$), lower Ki67 index ($P < 0.0001$) and a longer disease-free survival (DFS) and distant metastasis-free survival (DMFS) ($P = 0.0003$ and 0.0107). This association between a high AR expression and a good DFS and DMFS was significant for ER-positive tumors ($P < 0.0001$ and $P = 0.0018$); however, no association existed between AR expression and prognosis for ER-negative tumors. In patients ≤51 years old, a high AR expression level significantly correlated with a better prognosis, but this was not significant in patients who were 50 or younger. Multivariate Cox hazard analyses revealed AR expression to be independently associated with a good prognosis in overall patients (HR 0.46, $P = 0.0052$) and in the ER-positive cohort (HR 0.34, $P = 0.0009$). AR expression is associated with a less aggressive phenotype and a good prognosis in patients with ER-positive breast cancer. This is considered to be a specific phenomenon for postmenopausal breast cancer patients.

Introduction

The androgen receptor (AR) is a member of the steroid receptor subfamily. There is emerging evidence that the androgen signaling pathway may also play a critical role in normal and malignant breast tissue [1]. The AR is the most prevalent sex steroid receptor in malignant breast tumors, and is expressed in up to 90% of primary tumors and 75% of metastasis [2]. Previous studies revealed the expression of the AR to positively correlate with the estrogen receptor α (ERα) and progesterone receptor (PR) expression, low-grade, low proliferation activity, and advanced differentiation [3–11]. Several studies have demonstrated that the positivity for AR expression is associated with a better prognosis, especially in patients with ERα-positive breast cancers [1, 7–10]. In addition, the higher expression levels of the AR were associated with a better prognosis. This suggests that the AR may have a tumor-suppressive effect in breast cancer cells [1, 7, 9, 10]. Peters and colleagues showed that the AR is a direct repressor of ERα signaling in breast cancer cells [1].

Thus, the expression of AR is considered to be a good prognostic marker for ERα-positive breast cancer; however, there were some problems in previous studies. For example, the methods used to determine the positivity of

AR expression were different among the studies [3–11]. Moreover, even when the expression was assessed by immunohistochemistry (IHC), the cut-off value of the expression of the AR differed among the studies [1, 7–11].

The role of androgens in the development and progression of breast cancer has not yet been fully elucidated. The mechanism underlying estrogen production dramatically changes before and after menopause. In postmenopausal females, adipose tissue is the primary source of endogenous estrogen production, rather than the ovary. After menopause, androgens (which derive mainly from the adrenal gland) become an important source of estrogens [12]. The ratio of circulating estrogens and androgens changes drastically after menopause [13]. Thus, the role of androgens or the AR in breast cancer might differ by age or menopausal status. Although previous studies have examined the effects of androgen based on menopausal status, the relationship between the role of the AR and the age of breast cancer patients has not been reported previously. The present study investigated the expression of the AR by IHC and the relationship between AR expression and clinicopathological factors in primary invasive breast cancer. In addition, we evaluated the clinical significance of AR expression by age and ER status. In agreement with previous studies, AR expression correlated with less aggressive features in ER-positive breast cancer. We found that its expression is significantly associated with a less aggressive phenotype and a better prognosis in females aged 51 or older, but not significant in those who were 50 or younger, with ER-positive breast cancer.

Materials and Methods

Patient information

Four hundred sixty-six primary breast cancer patients underwent surgery in the Department of Surgery and Science, Kyushu University Hospital, between 1997 and 2007. Among these patients, eight had stage IV disease, 29 cases were non-invasive ductal carcinoma and 34 cases were a special type of invasive cancer. Among the remaining invasive ductal carcinoma cases, a total of 250 cases for which archival tissue samples were available for an immunohistochemical analysis were included in this study. Written informed consent was obtained from all patients before collecting tissue samples. AJCC/UICC TNM Classification and Stage groupings were used.

Immunohistochemistry to detect AR expression

The expression of the AR was analyzed by IHC. Formalin-fixed, paraffin-embedded tissue specimens were used, and the sections were deparaffinized with xylene and rehydrated. AR expression was analyzed as follows: The sections were first treated with the target retrieval solution (pH 9.0) (Dako, Glostrup, Denmark) in a microwave at 99°C for 30 min for antigen retrieval. The slides were then treated for 30 min with 3% H_2O_2 in methanol to block the endogenous peroxidase activity. Nonspecific antibody binding was blocked by incubating the sections with normal goat serum (Dako) for 10 min. The slides were then incubated with mouse monoclonal AR antibodies (AR441, diluted 1:50; Dako) [7, 9–11, 14] overnight at 4°C, and the samples were subsequently labeled with the Envision Detection System (DAB; Dako) for 1 h at room temperature. The sections were then developed with 3,3′-diaminobenzidine tetrahydrochloride (Dako) and counterstained with 10% Mayer's hematoxylin, dehydrated, and mounted. The expression of the AR was scored as the percentage of nuclear staining in a maximum of 1000 cells per sample.

Evaluation of ER, PR, HER2, and Ki67 expression

The ER, PR, and HER2 status was evaluated as described previously [15]. The ER and PR were considered to be positive if ≥1% of the nuclei of the tumor were stained by IHC [16–18]. Tumors were considered to be HER2-positive if they were scored as either 3+ on IHC or as 2+ on IHC with HER2 amplification (ratio > 2.0) detected by fluorescence in situ hybridization [16]. Ki67 was evaluated as described previously [19].

Statistical analyses

All molecular and IHC analyses were performed by investigators blinded to the clinical data. The statistical analyses were done using the JMP software package, version 9.0.2 (SAS Institute Inc., Cary, NC). The associations between AR expression and clinicopathological characteristics were assessed using χ^2 tests. Survival curves were plotted using the Kaplan–Meier method and the log-rank test was used to determine the associations between individual variables and survival. The survival data were evaluated using a multivariate Cox proportional hazards model. Differences were considered to be significant at $P < 0.05$.

Results

Expression of the AR detected by immunohistochemistry

AR expression levels were analyzed by IHC. AR immunoreactivity was observed in the nuclei of tumor cells.

Figures 1A and B show representative photographs of low and high expressions of the AR. The mean percent of AR expression was 71.1, the median percent was 83.8, and the range of AR expression was 0–99%. AR expression was higher in ER-positive cases compared with ER-negative cases (mean 78.6 ± 1.5% vs. 51.8 ± 3.9%, $P < 0.0001$; Fig. 1C), although the range of immunostaining in both groups was identical (0–99%). The Allred score of ER expression was available for 59 patients. In terms of the relationships between ER Allred score and

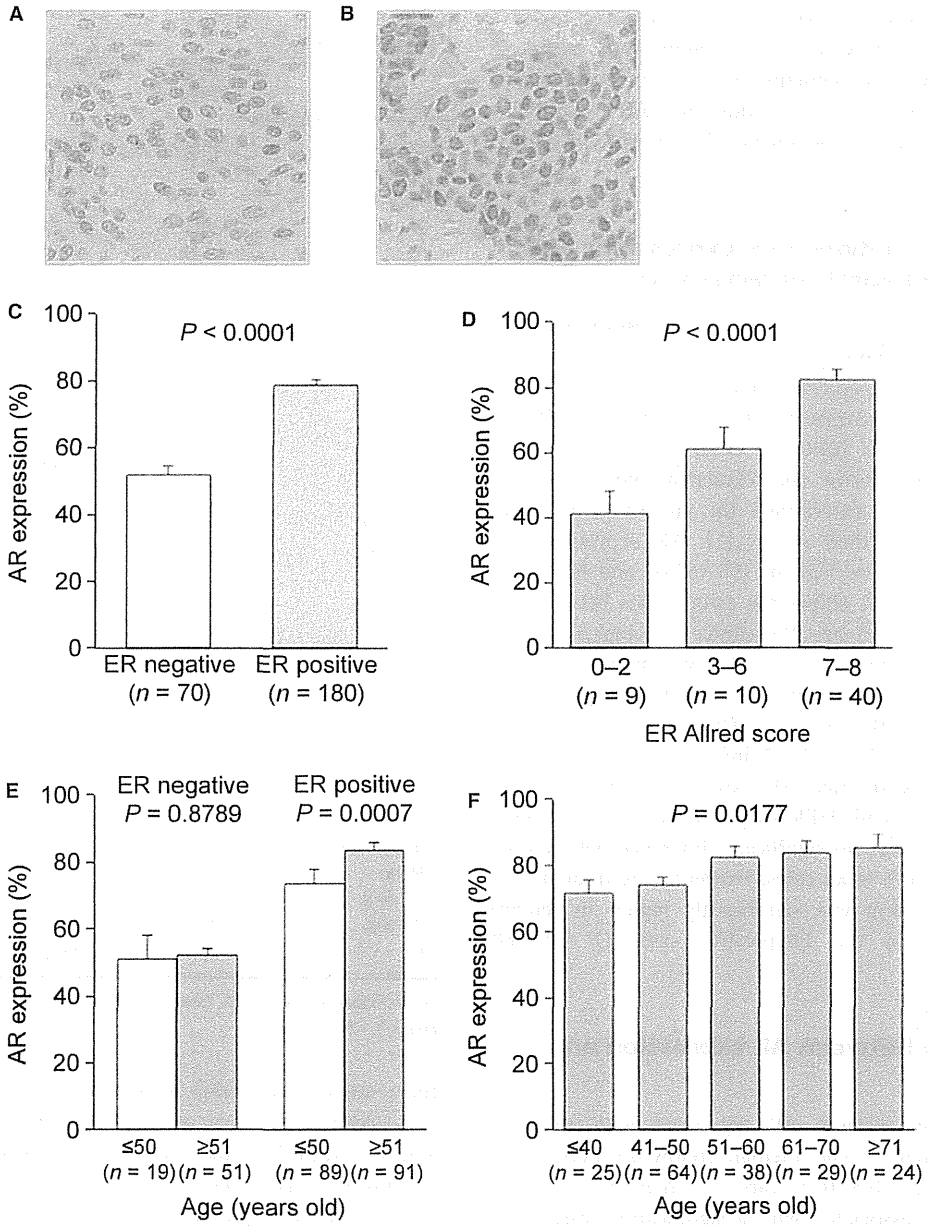

Figure 1. Results of the immunohistochemical analysis of androgen receptor (AR) expression levels in breast cancers. Representative images showing the negative (A) and positive (B) expressions of AR as evaluated by immunohistochemistry. Original magnification, 400×. (C) AR expressions were higher in estrogen receptor (ER)-positive breast cancer. (D) AR expression levels were associated with ER expression levels. (E) The relationship between AR expression and age in the ER-negative and ER-positive breast cancers. There were no significant differences in AR expression levels by age in ER-negative cases; however, AR expression was significantly higher in ER-positive patients who were 51 years old or older. (F) AR expression increased with age in the ER-positive cases.

AR expression, AR expression was higher when the ER Allred score was higher ($P < 0.0001$; Fig. 1D).

In addition, we found an intriguing phenomenon wherein AR expression was different by age only in ER-positive cases. The mean age at natural menopause in Japanese females is 50 years [20]. Therefore, we divided all of the cases into two groups by age: ≤50 and ≥51 years old. AR expression was similar in ER-negative cases in both age groups; however, it was significantly higher in the older group of patients with ER-positive cancer ($P = 0.0007$; Fig. 1E). In addition, AR expression increased with age in the ER-positive cases ($P = 0.0177$; Fig. 1F).

Associations between AR expressions and clinicopathological characteristics

The cut-off values used to classify AR expression were different among previous studies; however, the mean and median expression percentage and range detected in the current study are similar to those described in Peters' study [1]. Thus, in order to evaluate the associations between AR expression and clinicopathological factors and prognosis, we determined the cut-off value to be 75% according to their report [1]. AR expression was thus considered to be high in 155 (62%) and low in 95 (38%) cases. Table 1 shows the associations between the expression of the AR and the clinicopathological characteristics. High expression of the AR was significantly correlated with lower nuclear grade ($P < 0.0001$), ER and PR positivity ($P < 0.0001$ and $P = 0.0022$), HER2 negativity ($P = 0.0113$), and lower Ki67 index ($P < 0.0001$). Most of the tumors with high AR expression were hormone receptor-positive and HER2-negative cases ($P < 0.0001$; Table 1). There was no significant difference between age and AR expression in all cases. However, the frequency of high AR expression was significantly higher in females ≥51 years old in the ER-positive cases ($P = 0.0088$; Table 1).

Table 1. Associations between androgen receptor (AR) expression and clinicopathological characteristics.

	AR		
Factors	Low ($n = 95$)	High ($n = 155$)	*P*-value
Age			
≤50	45 (47.4)	63 (40.6)	0.2981
>50	50 (52.6)	92 (59.4)	
ER positive only			
≤50	32 (65.3)	57 (43.5)	0.0088
>50	17 (34.7)	74 (56.5)	
Lymph node metastasis			
Negative	54 (56.8)	90 (58.1)	0.8495
Positive	41 (43.2)	65 (41.9)	
Tumor size			
T1	39 (30.5)	80 (51.6)	0.1376
T2	49 (51.6)	60 (38.7)	
T3	7 (7.4)	15 (9.7)	
Nuclear grade			
1	29 (30.5)	81 (52.3)	<0.0001
2	19 (20.0)	40 (25.8)	
3	47 (49.5)	34 (21.9)	
ER			
Negative	46 (48.4)	24 (15.5)	<0.0001
Positive	49 (51.6)	131 (84.5)	
PR			
Negative	55 (57.9)	59 (38.1)	0.0022
Positive	40 (42.1)	96 (61.9)	
HER2			
Negative	69 (72.6)	133 (85.8)	0.0113
Positive	26 (27.4)	22 (14.2)	
Subtype			
HR+/HER2−	47 (49.5)	123 (79.4)	<0.0001
HR+/HER2+	7 (7.4)	12 (7.7)	
HER2	19 (20.0)	10 (6.5)	
Triple negative	22 (23.2)	10 (6.5)	
Ki67 index (%) (mean ± SE)	23.7 ± 1.5	14.2 ± 1.2	<0.0001
Adjuvant therapy in ER-positive cases			
None	2 (4.1)	13 (9.9)	0.1413
HT only	18 (36.7)	60 (45.8)	
CT only	15 (30.6)	22 (16.8)	
HT + CT	14 (28.6)	36 (27.5)	

ER, estrogen receptor; PR, progesterone receptor; HT, hormone therapy; CT, chemotherapy.

Association between AR expression and prognosis

The association between AR expression and prognosis was also evaluated. The median follow-up period was 6.6 years (range, 0.5–16.3 years). A high level of AR expression was associated with a significantly longer disease-free survival (DFS) and distant metastasis-free survival (DMFS) than a low AR expression ($P = 0.0003$ and 0.0107; Fig. 2A and B). This association between high AR expression and a good prognosis was significant in ER-positive tumors in terms of both DFS and DMFS ($P < 0.0001$ and $P = 0.0018$; Fig. 2C and D); however, there was no association between AR expression and DFS and DMFS in patients with ER-negative tumors (Fig. 2E and F). Regarding the adjuvant therapies prescribed in ER-positive cases, there were no significant differences between the AR-high and AR-low groups (Table 1).

Univariate and multivariate analyses were performed to assess the differences in DFS between the groups (Table 2). In addition to tumor size, lymph node metastasis, nuclear grade, HER2 status, and Ki67 index, AR expression was found to be significantly associated with DFS by univariate analysis. The multivariate Cox hazard

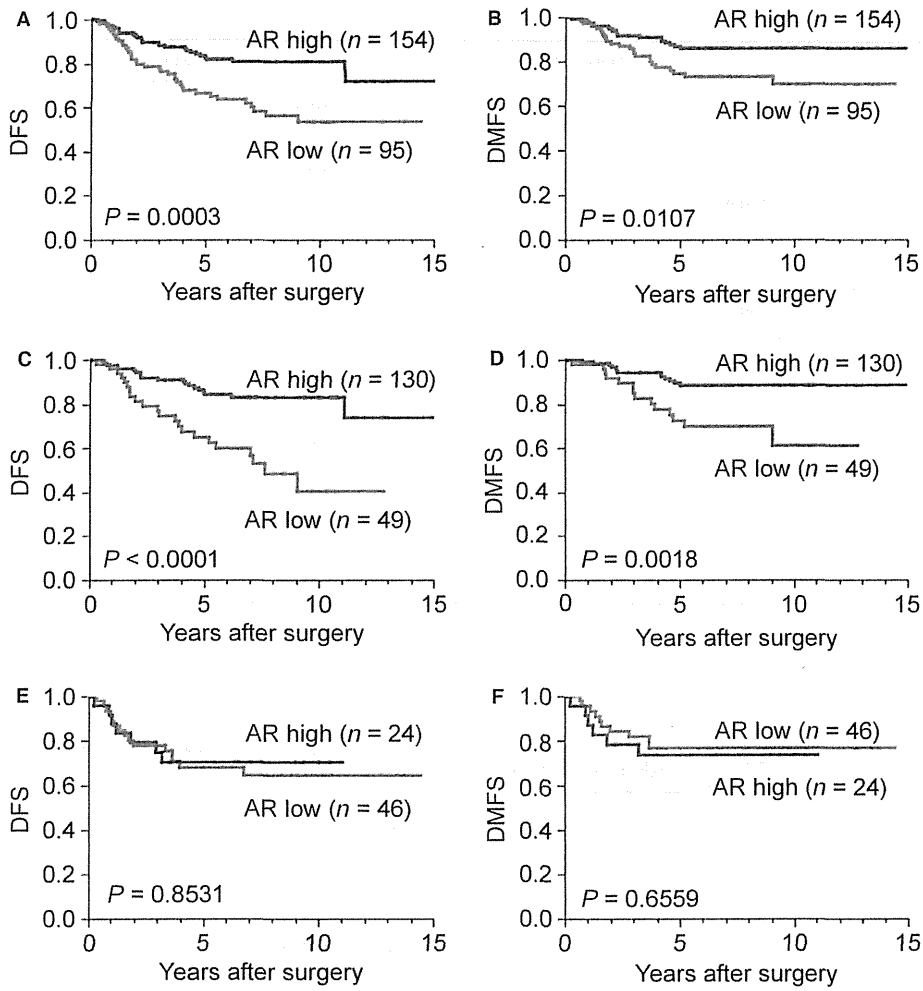

Figure 2. Relationship between disease-free survival (DFS) or distant metastasis-free survival (DMFS) and androgen receptor (AR) expression. (A and B) A high AR expression level was significantly associated with a longer DFS (A) and DMFS (B) in all cases. (C and D) A high AR expression level was correlated with a better prognosis in ER-positive cases in terms of both DFS (C) and DMFS (D). (E and F) No difference was observed in relation to AR expression in ER-negative cases in terms of both DFS (E) and DMFS (F).

analyses revealed that AR expression, as well as lymph node metastasis and nuclear grade, was independently associated with a good prognosis in the overall study population (high vs. low AR expression: HR, 0.46; 95% confidence interval, 0.26–0.79, $P = 0.0052$) and the ER-positive cohort of patients (high vs. low AR expression: HR, 0.34; 95% confidence interval, 0.18–0.64, $P = 0.0009$; Table 2).

Impact of the expression of the AR on the prognosis in ER-positive breast cancer by age

The percentage of tumor cells with AR expression differed by age in ER-positive cases (Fig. 1E and F). Therefore, the association between AR expression and prognosis was evaluated by age in the ER-positive cohort. In patients ≤50 years old, there was no significant association between AR expression and DFS and DMFS ($P = 0.1616$ and 0.0883; Fig. 3A and B). On the other hand, in patients who were 51 or older, a high AR expression level was significantly associated with a better prognosis in terms of DFS and DMFS ($P < 0.0001$ and $P = 0.0073$; Fig. 3C and D). Therefore, AR expression was considered to have a profound effect on the prognosis of older (51 years or older) females with ER-positive breast cancer.

In addition, the association between the prescribed adjuvant hormone therapy and the prognosis according to AR expression and age was investigated in ER-positive patients. In the ≤50-year-old group, the DFS of the

Table 2. Univariate and multivariate analyses for disease-free survival.

Factors		Univariate analysis			Multivariate analysis		
		HR	95% CI	*P*-value	HR	95% CI	*P*-value
All cases							
Tumor size	T3 vs. T1, T 2	2.67	1.32–4.92	0.0079	2.8	1.32–5.48	0.0082
LN meta.	Positive vs. negative	3.13	1.89–5.35	<0.0001	2.57	1.52–4.45	0.0004
Nuclear grade	3 vs. 1, 2	2.94	1.80–4.84	<0.0001	1.91	1.02–3.59	0.043
ER	Positive vs. negative	0.68	0.41–1.16	0.1545			
PR	Positive vs. negative	0.98	0.60–1.61	0.9443			
HER2	Positive vs. negative	2.25	1.30–3.76	0.0048	1.35	0.73–2.44	0.3261
Ki67	High vs. low	2.11	1.28–3.44	0.0036	1.12	0.61–2.04	0.7229
AR	High vs. low	0.41	0.25–0.68	0.0005	0.46	0.26–0.79	0.0052
ER-positive cases							
Tumor size	T3 vs. T1, T2	1.88	0.71–4.14	0.1863			
LN meta.	Positive vs. negative	3.29	1.76–6.45	0.0002	2.71	1.43–5.37	0.0021
Nuclear grade	3 vs. 1, 2	3.36	1.80–6.17	0.0002	2.37	1.25–4.43	0.009
PR	Positive vs. negative	1.60	0.80–3.57	0.1922			
HER2	Positive vs. negative	1.40	0.48–3.25	0.498			
Ki67	High vs. low	1.35	0.66–2.58	0.3915			
AR	High vs. low	0.30	0.16–0.54	0.0001	0.34	0.18–0.64	0.0009

HR, hazards ratio; CI, confidence interval; ER, estrogen receptor; PR, progesterone receptor; AR, androgen receptor; LN meta., lymph node metastasis; Ki67, cut-off 20%.

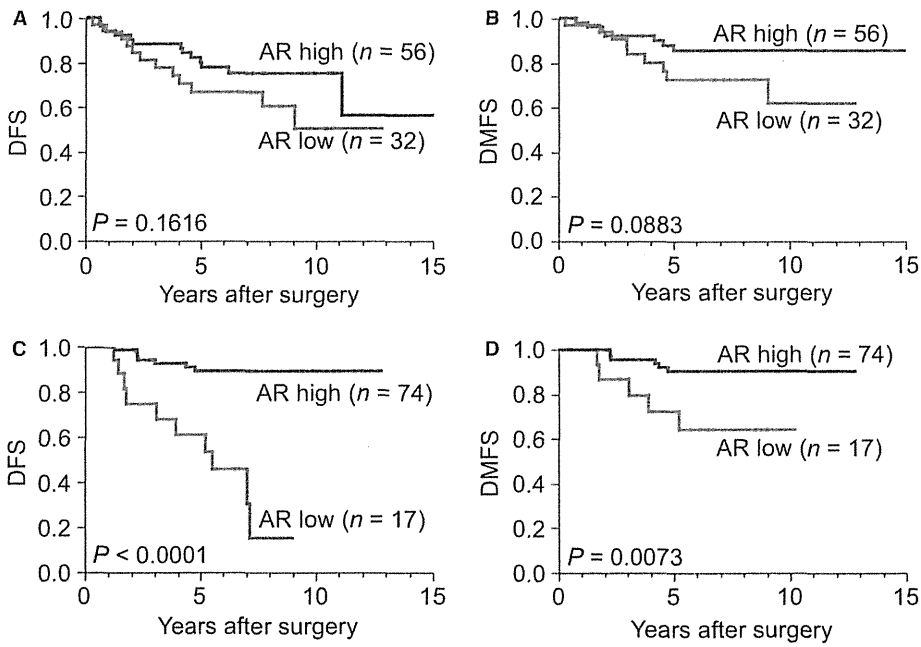

Figure 3. Impact of androgen receptor (AR) expression on the prognosis of patients with estrogen receptor (ER)-positive breast cancer by age. (A and B) In the younger (≤50-year-old) group, there was no significant association between AR expression and prognosis in terms of disease-free survival (DFS) (A) and distant metastasis-free survival (DMFS) (B). (C and D) On the other hand, in the older (≥51-year-old) group, a high AR expression level was significantly associated with a better prognosis in terms of both DFS (C) and DMFS (D).

patients treated with adjuvant hormone therapy was significantly better than that of the patients without adjuvant hormone therapy in both the AR-low and AR-high groups (P = 0.0030 and 0.0026; Fig. 4A and B). On the other hand, in females who were 51 years old or older, the DFS of the patients treated with adjuvant hormone